Bone microstructure under different loading environments

Beatrice Steyn

Department of Biological and Biomedical Engineering
McGill University, Montreal, QC
October 2021

McGill

A thesis submitted to McGill University in partial fulfillment of the requirement of the degree of Master of Engineering.

Abstract

Bone has the incredible ability to constantly adapt to its mechanical loading environment, adding new bone when loading is increased and removing bone in response to disuse and unloading. This study investigated the microstructure of bone under different loading conditions in two cases: 1) in response to controlled in vivo tibial loading of mice with a rare segmental progeroid disorder, gerodermia osteodysplastica (GO) caused by loss-of-function mutations in the *GORAB* gene. GO is associated with early onset osteoporosis and bone fragility; and 2) in response to housing conditions (conventional cages and high complexity aviaries) in commercial egg laying hens, who are known to develop disuse osteoporosis and keel bone fractures.

For Aim 1, our group previously observed that the long bones of *Gorab* conditional knockout mice ($Gorab^{Prx1}$) have a reduced mechanoresponse and a disrupted osteocyte lacunocanalicular network (OLCN) compared to littermates. Therefore, this study aimed to determine if the reduced mechanoresponse was primarily due to the loss of *Gorab* or a consequence of the developmentally altered OCLN. We compared the mechanoresponse in an inducible knockout mouse model of *Gorab* ($Gorab^{Prx1}$ iKO) with $Gorab^{Prx1}$. In vivo cyclic compressive loading was applied to the left tibia of 12-week-old iCre+ Gorab f/f female mice after the injection of tamoxifen (n=7, tamox) or vehicle (n=7, vehicle). The left tibiae underwent two weeks of loading (+1200με at midshaft determined by strain gauging, 216 cycles/day at 4 Hz, right tibiae non-loaded control). In vivo μCT of the tibia was performed (8 μm voxel size) at day 0, 5, 10, and 15. A volume of interest was selected as 5% of the tibial length at the midshaft of the tibia. Cortical bone data was analyzed at day 0 and day 15 using a repeated measure ANOVA and included cortical area (Ct.Ar), total area (Tt.Ar), cortical

thickness (Ct.Th) and principal moments of inertia (Imax, Imin). Measures reported as a change from baseline (day 15 – 0) demonstrated that loading led to increased Ct.Ar, Tt.Ar, Ct.Th, Imin and Imax in the loaded limbs of both the tamox and vehicle group. No significant interaction was measured, indicating that there was no difference in the cortical bone formation response to loading between the tamox and vehicle group. However, qPCR results revealed a *Gorab* knockout level of only 10% in femurs on the tamoxifen-treated group.

For Aim 2, a previous study showed that Lohmann Select Leghorn (LSL)-Lite pullets reared in specific high-complexity aviaries (HCA) had greater tibial bone density and strength than conventional cage (CC) reared pullets (Casey-Trott et al. 2017). Yet, although these aviaries allow for increased opportunity for physical activity during rearing, it is still unclear whether rearing in HCA influences keel bone microstructure. Therefore, this study aimed to determine whether hens with keel bone fractures have deleterious alterations to the keel bone microstructure, compared to those with intact keels. Furthermore, we aim to investigate if different rearing systems influence keel bone microstructure. Two flocks of Lohmann Selected Leghorn Lite (white) and Lohmann Brown Lite (brown) pullets were reared in CC and HCA until 17-weeks-of-age, after which, they were moved to furnished cages to begin the laying period. At 30-weeks-of-age birds from each genetic strain and housing system were randomly selected by palpation for keel bone fractures, radiographed and grouped as fractured (n =7) and non-fractured (n = 7) keel bones. Keel bones were excised, µCT-imaged (15 µm voxel size), and cortical and trabecular (trabecular number Tb.N, trabecular thickness Tb.Th, trabecular spacing Tb.Sp) microstructural parameters were assessed as in Aim 1. Fractured keel bones had greater Tb.Sp (42%) compared to non-fractured keel bones in both genetic strains and housing systems, although no significant differences were observed between the cortical parameters. Surprisingly, both cortical and trabecular microstructural outcomes were superior in CC compared to HCA across genetic strain and fracture status. Tt.Ar, Ma.Ar and Imin were greater in brown birds that in white birds, while Ct.Ar/Tt.Ar was lower in brown birds than in white birds.

In summary, my results showed that tamoxifen-treated mice with an intact OLCN respond to mechanical loading similarly to vehicle-treated mice. However, since qPCR results revealed that the *Gorab* gene was not successfully knocked out by tamoxifen treatment in these iKO mice, further studies are warranted. Therefore, a pilot study was started to test

different doses of tamoxifen treatment before the study can be repeated. Further my results showed surprisingly that both fractured and non-fractured keel bones have greater microstructural characteristics after CC-rearing compared to HCA-rearing. It may be evident that increased opportunity for exercise in high complexity aviary rearing do not have the same positive effect on keel bone characteristics as it has been shown to have on the radius, humerus and tibiotarsus of laying hens. Future studies examining whole bone geometry and material properties of the keel bones are needed to better understand the etiology of keel bone fractures.

Résumé

L'os a l'incroyable capacité de s'adapter en permanence à l'environnement mécanique auquel il est soumis, en ajoutant de l'os lorsque la charge est augmentée et en enlevant de l'os en réponse à l'immobilisation et à la diminution de charge mécanique. Cette étude a examiné la microstructure de l'os dans différentes conditions de charge dans deux cas : 1) en réponse à une charge tibiale controlee appliquée *in vivo* chez des souris atteintes d'un trouble progéroïde segmentaire rare, la gerodermie osteodysplastica (GO) causée par des mutations de perte de fonction dans le gene *GORAB*. La GO est associée à une ostéoporose précoce et à une fragilité osseuse; et 2) en réponse aux conditions d'hébergement (cages conventionnelles et volières complexes) chez les poules pondeuses commerciales, qui sont connues pour développer une ostéoporose d'immobilisation et des fractures du bréchet.

Pour l'objectif 1, notre groupe a précédemment observé que les souris où *Gorab* est délété spécifiquement dans les os longs ($Gorab^{Prx1}$) ont une mécano-réponse réduite et un réseau canaliculaire lacunaire d'ostéocyte (OLCN) perturbé par rapport aux souris contrôles. Par conséquent, cette étude visait à déterminer si la mécano-réponse réduite était principalement due à la perte de *Gorab* ou au fait d'avoir un OCLN altéré lors du développement. Nous avons comparé la mécano-réponse dans un modèle de souris knock-out inductible de *Gorab* ($Gorab^{Prx1}$ iKO) avec des souris $Gorab^{Prx1}$. Une charge compressive cyclique a été appliquée *in vivo* sur le tibia gauche de souris femelles iCre+ Gorab f/f âgées de 12 semaines après l'injection de tamoxifène (n=7) ou de véhicule (n=7). Le tibia gauche a subi deux semaines de charges (+1200με au milieu du tibia, déterminé par jauge de contrainte, 216 cycles/jour à 4 Hz, le tibia droit est utilisé comme contrôle non chargé). Le

µCT *in vivo* du tibia a été réalisé (taille de voxel de 8 µm) aux jours 0, 5, 10 et 15. Un volume d'intérêt consistant à 5 % de la longueur tibiale au niveau médian a été sélectionné. Les données sur l'os cortical ont été analysées au jour 0 et au jour 15 à l'aide d'une ANOVA à mesures répétées et incluaient l'aire corticale (Ct.Ar), l'aire totale (Tt.Ar), l'épaisseur corticale (Ct.Th) et les principaux moments d'inertie (Imax, Imin). Les mesures rapportées en tant que changement par rapport à la mesure basale (jour 15 - 0) ont démontré que la charge entraînait une augmentation des paramètres de l'os cortical (Ct.Ar, Tt.Ar, Ct .Th, Imin, Imax) dans les tibias gauches des Gorab^{Prx1} iKO injectés au tamoxifène et injectés avec le véhicule. Aucune interaction significative n'a été mesurée, indiquant qu'il n'y avait pas de différence entre le groupe injecté au tamoxifène et celui injecté avec le vehicule pour ce qui est de la réponse osseuse suite aux charges mécaniques. Cependant, les résultats de la qPCR ont révélé un niveau de knock-out de *Gorab* de seulement 10 % dans les fémurs.

Pour l'objectif 2, une étude précédente a montré que les poulettes Lohmann Select Leghorn (LSL)-Lite élevées dans des volières spécifiques à haute complexité (HCA) avaient une densité et une résistance osseuses tibiales supérieures à celles des poulettes élevées en cages conventionnelles (CC) (Casey-Trott et al. Poult Sci 2017). Pourtant, bien que ces volières permettent plus de possibilités d'activité physique pendant l'élevage, il n'est toujours pas clair si l'élevage en HCA influence la microstructure du bréchet. Par conséquent, cette étude visait à déterminer si les poules avec des fractures du bréchet présentaient des altérations délétères de la microstructure de cet os, par rapport à celles avec des bréchets intacts. De plus, nous voulons determiner si différents systèmes d'élevage influencent la microstructure de l'os du bréchet. Deux troupeaux de poulettes Lohmann Selected Leghorn Lite (blanc) et Lohmann Brown Lite (brun) ont été élevés en CC et HCA jusqu'à l'âge de 17 semaines, après quoi ils ont été transférés dans des cages enrichies pour commencer la période de ponte. À l'âge de 30 semaines, les oiseaux de chaque souche génétique et système d'élevage ont été sélectionnés au hasard par palpation pour les fractures du bréchet, radiographiés et séparés en deux groupes : bréchet fracturé (n = 7) et bréchet non fracturé (n = 7). Les bréchets ont été disséqués, analysés par µCT (taille de voxel de 15 µm), puis les paramètres microstructuraux corticaux et trabéculaires - nombre trabéculaire (Tb.N), épaisseur trabéculaire (Tb.Th), espacement trabéculaire (Tb.Sp) - ont été évalués comme dans l'objectif 1. Les bréchets fracturés avaient un plus grand Tb.Sp (42 %) par rapport aux bréchets intacts pour les deux souches génétiques et les deux systèmes d'élevage, bien

qu'aucune différence significative n'ait été observée pour les paramètres corticaux. Étonnamment, les résultats microstructuraux corticaux et trabéculaires étaient supérieurs pour les poules élevées en CC par rapport à celles élevées en HCA, indépendemment de la souche génétique et du statut de fracture. Les Tt.Ar, Ma.Ar et Imin étaient plus élevés chez les oiseaux bruns que chez les oiseaux blancs, tandis que le ratio Ct.Ar/Tt.Ar était plus faible chez les oiseaux bruns que chez les oiseaux blancs.

En résumé, mes résultats ont montré que les souris traitées au tamoxifène (qui devrait causer une deletion de *Gorab*), et donc ayant un OLCN intact, répondent au chargement mécanique de la même manière que les souris traitées au vehicule (où *Gorab* n'est pas délété). Cependant, étant donné que les résultats de la qPCR ont révélé que le gène *Gorab* n'a pas été éliminé avec succès par le traitement au tamoxifène chez ces souris iKO, d'autres études sont requises. Par conséquent, une étude pilote a été lancée pour tester différentes doses de tamoxifène avant que l'étude ne puisse être répétée. De plus, mes résultats ont montré de manière surprenante que les bréchets fracturés et non fracturés ont de meilleures caractéristiques microstructurales après l'élevage en CC par rapport à l'élevage en HCA. Il peut être évident que de meilleures possibilités d'activité physique dans l'élevage en volières de haute complexité n'a pas le même effet positif sur les caractéristiques du bréchet qu'il a été démontré qu'il avait sur le radius, l'humérus et le tibiotarse des poules pondeuses. De futures études examinant la géométrie de l'os entier et les propriétés matérielles du bréchet sont nécessaires pour mieux comprendre l'étiologie des fractures du bréchet.

Contents

Acknowledgements

Firstly, I would like to thank Dr. Bettina Willie for her guidance throughout the last two years. Although most of my time at the Shriners Hospital was during the COVID-19 pandemic, she still managed to provide me with ample learning opportunities and gave me opportunities to work on various projects. I am honored to have been a part of this lab and to have worked with exceptional lab mates, Isabela Vitienes, Alice Bouchard, Mahdi Hosseinitabataei, Maximillian Rummler, Kyle Kavaseri, David Bertrand, Celine Agnes and Taylor deVet. I would like to especially thank Catherine Julien, for her patience to train me and for her kindness to always answer all my questions.

I could not have presented this work without the help of our summer students, Samantha McCluskey, Gabrielle Graceffa and Carolyn Denton. Thank you for your endless support in dissecting chickens, for bringing me supplies when I had to quarantine (Gabrielle) and for helping to transport chickens (Samantha).

I would also like to thank Pina Sorrini from the McGill Biological and Biomedical Engineering faculty for her support and guidance through the uncertain times of the pandemic.

Finally, I would like to thank my family in South Africa and housemates in Montreal for supporting me academically, financially, and mentally. I am immensely grateful to have such a support network that motivates me to achieve my academic goals.

Contribution of Authors

Chapter 1 (Background and Rationale) were completed by Beatrice Steyn and revised by Dr. Bettina Willie.

Chapter 2 (Mechano-adaptation in *Gorab* inducible knockout mice)

- B. Steyn – performed all microCT analysis, statistical analysis, histomorphometry, gene expression analysis
- C. Julien – performed loading experiments and microCT imaging, assisted gene expression analysis.
- W.L Chan – contributed to study design, supplied animals
- U. Kornak- contributed to study design, supplied animals
- B. Willie – study design, supervisory support, funding procurements, performed loading experiments.

Chapter 3 (The effect of rearing housing system on the keel density and microstructure in egg-laying hens)

- B. Steyn – performed all surgical procedures, microCT imaging, microCT analysis, statistical analysis
- I. Vitienes – assisted all surgical procedures and experiments.
- C. Denton – assisted surgical procedures
- A. Bouchard – assisted surgical procedures
- S. McCluskey – assisted surgical procedures
- B. Willie – study design, supervisory support, funding procurements

In addition to the manuscripts that will result from the research presented in chapters 2 and 3 of this thesis, I also contributed on several other projects:

- Hosseinitabatabaei S, Mikolajewicz N, Zimmermann EA, Rummler M, **Steyn B**, Julien C, Rauch F, Willie BM. 3D image registration marginally improves the precision of HR-pQCT measurements compared to cross-sectional-area registration in adults with osteogenesis imperfecta. Journal of Bone and Mineral Research, Submitted 07-2021. – Performed image registration

- Ziouti F*, Rummler M*, **Steyn B**, Thiele T, Seliger A, Duda G, Bogen B, Willie BM#, Jundt F#, (* #,,shared authorship). Prevention of bone destruction by mechanical loading is not enhanced by the Bruton's tyrosine kinase inhibitor CC-292 in myeloma bone disease. International Journal of Molecular Sciences, 7;22(8):3840, 2021. – performed histomorphometry

- Vitienes. I, Ross. E, Graceffa. G, Bouchard. A, **Steyn. B**, Widowski. T, Willie. B. Aviary rearing enhances bone microstructure in Lohmann LSL-Lite and bone mass in Lohmann Brown Lite egg-laying hen pullets compared to conventional cage-rearing. In preparation – performed microCT analysis

List of Figures

List of Tables

Chapter 1

Background and Rationale

1.1 Bone

The mechanical support and protection that bones provide, are a critically important function of bone. Besides being load bearing, bone can also adapt their structure to the local loading environment, i.e. repetitive loading, to avoid fractures [1]. This adaptation is possible because of the multiscale organization of bone that allow for the transduction of mechanical stimuli [1].

1.1.1 Bone Biology

The primary cells in bone consist of osteoclasts, osteoblasts, and osteocytes. These bone cells are responsible for bone modeling, the formation of new bone, and bone remodeling, the replacement of damaged bone [2]. Osteoclasts are the primary cells responsible for bone resorption and are recruited to sites to remove damaged bone or bone with microfractures.

Osteoblasts are the bone forming cells that originate from mesenchymal progenitors. After these osteoblasts secrete bone matrix protein and mineralize bone, they either remain

entrapped in bone as osteocytes, become bone lining cells, or die by apoptosis [2]. The two major signaling pathways that regulate osteoblasts are transforming growth factor beta (TGF-β) / bone morphogenic protein (BMP) signaling and Wnt signaling. Increased Wnt signaling leads to increased osteoblasts which results in increased bone formation [2]. The number of osteoblasts in bone can also be increased by decreasing the rate of their apoptosis [2].

Of these three bone cell types, the osteocyte is the most abundant, making up 90-95% of all bone cells [3]. Osteocytes were previously viewed as inactive cells, however, this observation changes drastically in the last 15 years, with research proving that osteocytes play several roles in the skeleton [3]. Now, osteocytes are known as the orchestrators of bone (re)modeling, regulating osteoblast and osteoclast activity, phosphate homeostasis and sensing mechanical loading [3], [4], [5]. Osteocytes play a key role in controlling osteoblasts and osteoclasts through sclerostin and osteoprotogerin regulation, as well as in bone mechanotransduction [3], [4]. Studies propose that osteocytes apoptosis occurring at sites of microdamage, stimulates osteoclast activity to remove dead osteocytes. Noble et al. further showed that mechanical loading, within the physiological range, produce strain that can decrease the levels of osteocyte apoptosis, while high levels of loading can cause damage to the bone and leads to increased apoptosis [6].

1.1.2 Bone Structure

The bone structure can be organized into macro-, micro-, and nanostructure. The macrostructure includes dense cortical bone, porous trabecular bone and creates four skeletal envelopes: 1) periosteal, 2) intracortical, 3) endocortical and 4) cancellous upon which bone cells can act [1]. The shaft or diaphysis of long bones primarily consists of compact cortical bone that provides both support and protection. At the end of long bones, in the metaphysis, trabecular bone also provides support but, most importantly, it redirects stresses to the stronger cortical shell [1].

The microstructure consists of collagen and mineral matrix, organized for specific functional need. During pathologic situations, normal skeletal development and when bones experience higher than normal mechanical loads, woven bone are rapidly formed that

primarily acts as a repair tissue [1]. While woven bone is highly disorganized, primary bone is arranged in a lamellar pattern and consists of primary lamellar bone, plexiform bone and primary osteons [1]. Primary lamellar bone is formed on the periosteal and the endosteal, while plexiform bone is mostly only found in animals, not humans [1]. Whereas primary bone is the formation of new bone, secondary bone is the repair and replacement of previously deposited damaged bone.

The nanoscale organization of bone includes collagen fibers and non-collagen extracellular matrix proteins (NCPs) [1]. Research has shown that these collagen fibers are oriented with respect to the stress in the bone, longitudinally in bones under tension, and transversely in bones under compression [1]. The nanostructure also consists of organic and mineral components that make up bone microstructures and provide bone resilience, ductility, and stiffness. These minerals are deposited in the gaps between the collagen fibrils during primary and secondary mineralization. Initially, mineral deposition within the collagen framework increases rapidly and reaches 70% of mineralization within three weeks, whereas secondary mineralization is a much slower and continuous process over months or years. These minerals are released through bone remodeling and distributed via the extensive osteocyte lacunae and canalicular channels [1]. Although NCPs only make up 2% of bone, they play a vital role in regulating and directing the maintenance and construction of the extracellular matrix. They also control mineralization and regulate the size and formation of collagen fibers [1].

1.1.3 Bone Biology and Structure in Mice

Among animals commonly used for biological research, the laboratory mouse (Mus musculus) is the most highly utilized animal to advance our knowledge of human physiology [7]. Due to the short gestation period of mice and physiological similarity to humans, scientist can investigate in vivo situations of bone cells to address fundamental questions regarding bone formation, remodeling, and function. Since we used C57BL/6 mice in our study, we will focus on the similarities and differences between C57BL/6 mice and human bone biology.

The average life span is 866 days for female C57BL/6 mice and 901 days for male C57BL/6 mice [8], which is a relatively long life span, making these mice ideal models for age-related bone loss studies. These mice reach sexual maturity at six to eight weeks of age. While human bone acquisition and longitudinal bone growth cease with the onset of puberty, it continues in mice after sexual maturity, with peak bone mass achieved at four to six months of age [9]. This is evident in the growth plate of long bones, where, in humans, the metaphysis and epiphysis fuses and the growth plate vanish, while in mice, the growth plate does not fuse or disappear [10]. Although the growth plate was still present and peak bone mass was achieved at 6 months of age, C57BL/6 mice showed no change in femoral length between 6 to 12 months of age [11]. Furthermore, while human cortical bone has blood vessels and osteons, murine cortical bone lacks osteons [12]. Therefore, mice bones rarely undergo secondary, also called intracortical, remodeling [13], but instead experiences surface remodeling. While trabecular bone turnover in the iliac crest of humans is about 0.1% per day [14], mice femurs showed a bone turnover rate of 0.7% per day [15]. At these rates, mice complete a cycle of bone remodeling every two weeks [15] and humans every six to nine months [16], which is in accordance with the higher metabolic rate of small animals. Similarities in bone loss have also been reported, with C57BL/6 mice and humans showing cancellous bone loss beginning in early adulthood [11], [17], [18]. At three months of age, femoral cancellous bone started to decline and almost completely vanished by 8 to 12 months of age in both mice sexes. Interestingly, both human and mice age-related bone loss are associated with reduced trabecular number and connectivity, while humans also show a reduction in trabecular thickness [11], [18], [19].

1.1.4 Bone Biology and Structure in Chickens

The poultry industry has been a major global industry, known for breeding chickens for their meat and eggs. The modern laying hen, descendant from the red jungle fowl, is genetically selected for efficient egg production [20]. Besides genetic strain, various factors play a role in the welfare of these laying hens, therefore extensive research in the poultry industry is needed. Soon after the introduction of battery cages (Couch, 1955), caged layer fatigue or paralysis, associated with weakened skeleton and osteoporosis, was identified as

a major welfare concern. Poor skeletal health in these chickens were first observed in the 1930s, which led to non-cage systems becoming more common [21]. Later, high laying performance and the development of modern laying strains lead to commercial laying farms from across the globe reporting that 70 to 97% of their hens suffer from keel bone deformities at the end of lay [22], [23], [24], [25]. To investigate the physiological effects of these factors, it is important to understand the bone biology and bone microstructure of chickens.

Similarly to mammalian bone, osteoblasts are bone-forming cells that produce bone matrix and bone-resorption osteoclasts are responsible for bone remodeling. During growth, called the rearing period, bones elongate by continued proliferation of chondrocytes at the head of the growth plate. These growth plates are much better vascularized than mammalian ones and does not involve a secondary ossification center [26]. Towards the end of the rearing period, osteoclast remodeling activity increases and form secondary osteons. During this process, osteoblasts become entombed within the bone, differentiate into osteocytes, form an intrinsic interconnected network and respond to mechanical stimuli as in mammalian bone [26].

After the rearing period, hens are sexually mature and enter the laying period, in which their bone biology changes drastically to accommodate for egg production. Therefore, besides cortical and cancellous bone, laying hens produce medullary bone during the laying period, that is primarily produced to facilitate adequate calcium supply for rapid calcification of eggshells. To facilitate medullary production, osteoblast activity shifts to forming woven medullary bone instead of structural lamellar cortical bone [26]. This shift is stimulated by estrogen, a hormone that rises considerably at the onset of sexual maturity [26]. Even though the osteoblast activity cease to form cortical bone, osteoclasts continue to resorb both cortical and medullary bone during the laying period, which results in declined structural bone throughout the skeleton, including the keel bone [26]. Although it is believed that medullary bone replaces the resorbed cortical bone, it does not supply the same structural supports, thus resulting in a fundamentally weaker skeleton associated with increased fracture risk and osteoporosis [26]. Thus, the role of estrogen levels in osteoporosis in laying hens is in contrasts with that in post-menopausal women, where reduced estrogen levels lead to osteoporosis.

The ossification process of the keel bone is also significantly different than that of long bones. While intramembranous ossification is involved in the widening of long bones, endochondral keel bone ossification starts in the cranial region and progresses towards the caudal tip [27], [26]. Also, while long bone growth ceases at the onset of lay (16 to 18 weeks of age), keel bone ossification continues until 28 to 40 weeks of age [26]. It is also still unclear where medullary bone is primarily deposited within the keel bone. Previous work distinguished that avian medullary bone is primarily deposited in the mid-shaft of avian long bones, with cancellous bone concentrated in the metaphysis region, but none report on how to distinguish between cancellous bone and medullary bone within the keel bone [28].

1.2 Bone adaptation to mechanical loading

Bones have the incredible ability to form new bone, to replace damaged bone and to adapt to mechanical loading to meet functional demands [1]. The human skeleton is constantly adapting to its mechanical loading environment through adaptive (re)modeling, adding new bone when loading is increased and removing bone in response to disuse and unloading [3]. The Wolff law explains the relationship between the internal skeletal structures of bone and mechanical stress [29]. It describes that trabeculae are aligned with the stress direction and that this adaptation is a dynamic and self-regulating process [29]. The Wolff law uses strict mathematical laws to explain why increased bone mass is seen in areas of high mechanical stress and low bone mass is seen in areas experiencing low mechanical stress [30]. This relationship has been studied by investigating bone macro- and microstructures, including bone length, cortical thickness, cross section geometry and bone curvature.

1.2.1 Mechanotransduction

The mechanotransduction process starts by 1) osteocytes sensing the mechanical stimuli, and then 2) osteocytes transmit biochemical signals that lead to 3) effector cell response.

Ideally, the bone cells responsible for sensing mechanical forces should be widely distributed throughout the bone matrix and extensively interconnected to ensure sufficient mechanotransduction. Osteocytes are believed to be the key bone cells responsible for sensing mechanical strain, due to their intricate network of cell bodies being located inside fluid-filled lacunae and being connected to both osteoblasts and bone-lining cells [3]. When this interstitial fluid flow experience mechanical strain, it can deform the osteocyte. It remains unclear exactly how the osteocyte detects mechanical signals or what magnitude of fluid flow is necessary to induce osteocyte response. Besides sensing the fluid flow shear stress, osteocytes are also considered to coordinate bone modelling and remodeling by signaling the activity of the bone-forming osteoblasts and bone-resorbing osteoclasts in response to loading [31]. Recent studies suggests that osteocytes send signals inhibiting osteoclast activation when bones are loaded [3]. These signals include the regulation of sclerostin, which is an osteoblast inhibitor, and osteoclastogenic cytokine receptor activator of nuclear factor kB ligand (RANKL), which is produced by under- and over-stimulated osteocytes. Sclerostin is downregulated in osteocytes during loading and upregulated during unloading [32]. Tissue microdamage leads to osteocyte apoptosis and the release of RANKL which in turn promotes osteoclasts to the damaged tissue site [33]. Osteoclast resorption initiates osteoblastic bone formation which replaces the damaged bone tissue. In humans, this remodeling primarily occurs within the cortical bone whereas rodents show remodeling on bone surfaces (endocortical, periosteal and trabecular).

Another property that influences mechanoresponse is the material properties of bone, which includes the organization of vascular canals, the orientation of collagen fibers, the composition and nano-scale organization of bone. One of these nano-scale organizations is the osteocyte lacunocanalicular network (OLCN), formed by the interconnection of osteocytes embedded in mineralized bone tissue [29]. This extensive network is thought to be responsible for the flow of interstitial fluid to produce osteocyte mechanical stimulation,

to provide the osteocytes with metabolic substrates and to remove their waste [29]. Research suggests that osteocytes can add and remove minerals from surrounding lacunae and canaliculi, which can affect the lacunar size and matrix properties [34]. These modifications could result from changes in mechanical loading [35]. Since the surface area of the lacunar network is greater than the bone surface area, even the smallest change can affect the bone properties and the fluid flow shear stress on the osteocyte [3]. It has been shown that osteocytes and their lacunae vary in shape depending on the anatomical location and age of the bone, which has been hypothesized to affect mechanotransduction [35]. An altered OLCN may impair the mechanoresponse of bone.

1.2.2 Mechanoadaptation in Humans

One of the simplest ways to increase the mechanical loads on skeletal bones is to increase the level of exercise. In terms of external loads experienced during exercise, high strain rates, like jumping, creates a greater osteogenic effect than constant loads, like walking. It is clear that only a few (< 40) loading cycles, divided into shorter bouts with rest periods, are necessary per day to elicit adaptive responses [36]. Several human exercise trials demonstrate that the skeleton of children and adolescents are capable of greater structural adaptation to mechanical stimulus, compared to the adult skeleton [37]. Physical stimuli in young people enhances osteogenesis more effectively than in older people [36], [38].

Besides gravitational forces that bone experience during exercise, Frost proposed that voluntary muscle forces dominate the structural adaptations of bone to mechanical usage [39]. Muscle forces place greater loads on bone than gravitational forces associated with weight [40], [41]. Multiple studies have demonstrated that greater muscle mass/strength is associated with greater bone mass [42]–[45]. Sievanen's natural experiment also supported Frost's argument that the loss of muscle strength during disuse, precedes the loss of bone and that muscle mass respond more rapidly than bone to changes in mechanical environment [44]. Frost further explained bone's "stiffness lag", which described the delay between bone formation and fully mineralized mature bone [46]. These differences in muscle and bone's response to loading become evident in rapidly growing adolescents who will avulse their tibial tubercle during activity. For a period of time, active adolescents' muscle strength increases

more rapidly than their growing bone, which causes their muscles to pull with greater force, that can cause avulsion fractures [47].

These principals have been researched more extensively in mice due to the low cost of these animal models and their short lifespans.

1.2.3 Mechanoadaptation in Mice

In vivo, tibia loading in mice have been used to assess bone adaptation and mechanotransduction in about a hundred published studies [48]. One common mouse loading model is the axial compression tibial loading model, in which compressive loads are applied along the length of the tibia [49]. The benefits of this model are 1) that a controlled load can be applied and isolated to a targeted limb, so that the load can be described and quantified unlike exercise models, 2) that the contralateral limb can act as a within-animal control, and 3) that both cancellous and cortical bone adaptation can be studied. Further, this model can be used to investigate single, continuous, static, and dynamic loading conditions by adjusting the load cycles and waveform. These different loading conditions stimulate different bone activities. Dynamic loads, repeated daily for 1 to 2 weeks, are required for mineralized bone formation [50]. Also, a strain magnitude higher than the minimum effective strain to stimulate bone formation needs to be attained during loading [48]. Standard methods used to measure the outcomes of these loading studies are microcomputed tomography (μCT) and histomorphometry. Changes in the bone microstructure from baseline can be quantified by in vivo μCT scan analysis, while fluorochrome labeling allows for bone formation evaluation. Using these methods, animal loading studies has shown that loading has a much greater effect on formation than on resorption of trabecular bone [51].

In terms of mouse genetic strains studied in the axial compression tibial loading model, C57Bl/6 and BALB/c mice are the most used. Several studies have reported the bone formation response to loading in these mouse models, in both sexes and in young and matured mice. In summary, six-week-old female C57Bl/6 mice and female BALB/c mice showed greater cortical bone volume than their age-matched controls [52] and both genetic strains showed reduced bone formation response to loading with aging [53]–[56]. Twenty-

two-month-old male BALB/c mice showed a greater response to loading than seven month old male BALB/c mice at the endocortical surface [57]. Different loading protocols with different waveforms have also shown to influences tibial adaptation to loading more than genetic strain [52], [48].

Besides investigating age- and genetic strain-related mechanoresponse, this loading model can also be utilized to investigate bone mechanoresponse in genetic bone diseases since conditional knock-in/knock-out mice models are well developed. These mice models contribute significantly to understanding genetic mutations and to develop therapies to treat bone diseases, like osteoporosis, in humans.

Not only is osteoporosis a common bone disease in humans, but it is also a major welfare concern in commercial egg-laying hens. Although many studies have described mechanoadaptation of the mammalian skeleton, few assess the effects of mechanical loading on the avian skeleton.

1.2.4 Mechanoadaptation in Chickens

When considering the overall skeletal health of laying hens, it is essential to take other factors, besides the biological changes occurring with sexual maturity, into account. These factors include diet, genetic strain, and daily activity, which all play a role in the mechanoadaptation in chickens.

Part of the eggshell calcium (25 to 40%) comes from the skeleton and the other part from the diet [58]. Mueller reported the calcium metabolism in pullets that receive a constant specific activity ration for 26 days and showed that 78% of dietary calcium intake was absorbed and 70% of the absorbed calcium was retained. With the increased demand for shell formation, a significant increase in calcium retention was observed, with more calcium mobilized for bone and shell deposition [59]. It has also been shown that hen's capacity to absorb calcium has a threshold, and that calcium levels beyond this threshold does not improve bone health but can even lead to kidney lesions [60]. Efforts have also been made to prolong the period of availability and retention of calcium from the diet [60].

The effect of inheritable bone characteristics must be considered when investigating osteoporosis in laying hens. Commercially, Lohmann White and Lohmann Brown birds are the most common strains used in Canada. A study conducted on white birds reported that tibial strength, humeral strength, and keel radiographic density were moderate to strong heritable characteristics [61]. Therefore, genetic strain plays a role in avian osteoporosis, with certain strains having bone traits that reduce the risk of bone fractures in laying hens [61].

A major welfare factor to consider is the housing and associated activity of laying hens. Although limited research has been done on the effects of exercise on bone formation and resorption in laying hens, studies have reported that hypoactivity or confinement leads to bone loss and reduced bone mineral density in both the femur and tibia of pullets [62]. Because the rearing period is the crucial stage for skeletal development, pullets should be allowed to perform natural activities, like pecking, perching, wing flapping and running during this period [63]. Interestingly, a study reported that white-feathered birds (Lohmann LSL Lite) performed more wing-associated locomotor behavior than brown-feathered birds (Lohmann Brown) [64]. Rearing housing styles that allow for these natural activities and opportunities for mechanical loading have been reported to benefit bone growth in pullets [60]. Also, most studies on the mechanoadaptation in chickens investigated the tibiotarsus of laying birds housed in different housing systems. These housing systems range from conventional cages (CC) to free-range, with aviary systems of different complexities in between. A method used to encourage activity is providing perches within rearing housing, which was reported to increase bone mineral content of the tibia as well as increased leg muscle and body weight [60].

A study on 16-week-old Lohmann Selected Leghorn-Lite (LSL-Lite) pullets reported that pullets reared in aviary systems had a longer keel metasternum and caudal tip cartilage length compared to pullets reared in conventional cages [63]. Regarding the keel bone characteristics, no major differences were reported between the different rearing systems [63]. Interestingly, the tibiae and humeri of aviary reared 77-week-old Lohmann White hens showed significantly greater cortical thickness and density than hens reared in conventional cages [65]. This suggests that restricted movement during rearing causes loss in tibia bone mass and density towards the end of lay. Whether rearing housing has a similar long-term effect on keel bone characteristics than on the microstructure of the tibia is still unclear.

To better understand what type of loading is exerted during flight on the wing and surrounding bone structures, like the keel bone, it is important to gain knowledge on the biomechanics of bird flight. The primary flight muscles of birds are the pectoralis and supracoracoideus, which are designed to withstand large stress and strain conditions during flight [66]. The pectoralis is the largest wing muscle and the primary downstroke muscles, whereas the supracoracoideus is responsible for primary upstroke [66]. The pectoralis major and minor are anchored to the keel bone and insert upon the humerus and account for the largest mechanical power output from the muscles for flight [67]. Sokoloff et al. has confirmed that the supracoracoideus is not necessary for birds to take-off and fly [68]. The pectoralis is designed to produce work and power and undergoes large changes in length (muscle strain) during contraction (up to 40% of resting length) [69], [70]. Although, birds use different methods to produce flight power, therefore pectoralis strain varies among flight modes and bird species [67], [71], [72]. More specifically, it is unclear how pectoralis strain varies in chickens, especially laying hens.

Muscle forces place greater loads on bone than gravitational forces in humans [40], [41]. Since the pectoralis muscle is the largest wing muscle and it is anchored to the keel bone, it is believed to exerts a force on the keel bone during wing-flapping, similarly to human exercise studies previously mentioned. Pectoralis strain varies in different birds and during different activities, so the magnitude of the load exerted on the keel bone is still undetermined. How this force, during wing-flapping, affects the keel bone microstructure is also still unclear. While most studies investigate bone biology and mechanical strain of chicken long bones like the tibiotarsus, little is known about the etiology of keel bone fractures which is a major welfare concern.

1.2.5 Osteocytes in Aging and Disuse

Age-related bone loss refers to reduced bone turnover due to changes in energy metabolism that occurs as a function of aging [1]. Age-related osteoporosis is a global health burden, with around nine million osteoporotic fracture cases per year [35]. Hence, extensive research has been invested to better understand the underlying cause of low bone mass and deteriorated bone microstructure that leads to reduced bone strength and increased risk of

fragility fractures [35]. Although age-related bone loss may be caused by reduced skeletal loading [73], [74] which is also associated with reduced muscle mass [47], [75], [76], studies show that these are not the primary factors of age-related bone loss. Reduced bone strength associated with aging/osteoporosis may be due to the reduced or diminished ability of bone to adapt to changes in mechanical loading environments. Several human studies [77]–[86] and experimental animal studies [87]–[96] supports this suggestion.

This reduced ability to adapt to mechanical environments leads to changes in the bone structure and material properties, as demonstrated in postmenopausal women and aged men with increased bone resorption rates compared to bone formation rates [97], [98]. This creates an imbalance in cell activity, causing more bone to be resorbed and ultimately leading to lower bone mass. Interestingly, this phenomena has a greater effect on trabecular bone loss than cortical bone loss in humans before the age of 50 [99]. In an animal study, C57Bl/6J mice showed reduction in trabecular bone volume from 6 to 8 weeks of age, while cortical bone only started to decrease slightly after 3 months of age [11].

Besides bone's reduced ability to adapt to changes in mechanical environment, studies have suggested that bone's reduced capacity to sense or respond to loading may in part contribute to age-related bone loss [100]. Deterioration of the osteocyte lacunocanalicular network has been observed with aging [101]–[103]. Deterioration of the network is a possible mechanism causing reduced mechanoadaptation. Decreased levels of osteocytes has been reported to be associated with aging. More specifically, collagen formation and the width of preosseous and osteoid zones became diminished with aging [104]. The frequency of forming osteons and incompletely mineralized osteons increased with age, which suggests that protein matrix synthesis by osteoblasts decrease with aging and that initial mineralization, mediated by osteoblasts and osteocytes, becomes increasingly deficient with aging [105]. Tatsumi et al. described how targeted ablation of 70 to 80% of osteocytes in a mouse model exhibited fragile bone with microfractures, osteoblastic dysfunction, trabecular bone loss and intercortical porosity, all of which are associated with aging and osteoporosis [5].

A recent study by van Tol et al. showed that osteocyte network architecture is a key determinant of bone (re)modeling [106]. They showed that fluid flow shear stress based on the osteocyte lacunocanalicular network architecture was a better predictor of bone

formation and resorption than strain. Thus, defective osteocyte lacunocanalicular network architecture likely plays a role in bone health.

In addition to age-related osteoporosis, bone loss during disuse, like bedrest or microgravity during spaceflight, is also a major concern. Gravity plays an important role in both the development and maintenance of bone mass. Both humans and animals demonstrate intense bone loss in weight-bearing bones after extended periods of microgravity in spaceflight. A JAXA mission in which 8-week-old male mice were subjected to spaceflight for a month, showed significant decrease in femoral trabecular bone mass [107]. It remains unclear what causes the reduces bone mass, so another mission, including 20-week-old male mice, performed histological analysis and found that osteoblast surface/bone surface was reduced while osteoclast surface/bone surface was elevated [108]. Further, this study also reported decreased trabecular bone volume, reduce osteocyte lacunae volume, more spherical shape osteocytes and increased empty lacunae. It suggested that spaceflight induces osteocyte death and that the increased presence of dead osteocytes drastically promotes osteoclast activity which is responsible for the deterioration of bone [108].

Few studies have investigated the effects of microgravity on bones like the sternum. Nine-week-old male C57BL/6 mice showed no changes in sternum microstructure between spaceflight and ground control groups. Disuse osteoporosis is a major welfare concern in laying hens, especially those housed in conventional cages (CC), where they experience prolonged and severely limited ability to walk of perform any physical activity. Not only does CC reduce weight-bearing activities, but it also reduces strain on the non-weight bearing bones like the wings and keel, due to restricted wing flapping [109].

Hypothesis and Aims

Study 1 - Mechano-adaptation in *Gorab* inducible knockout mice

The aim of this study was to determine if the reduced mechanoresponse of Gorab^{Prx1} mice previously observed [110] was primarily due to the loss of the *Gorab* gene or a consequence of the developmentally altered OCLN. We aimed to compare the mechanoresponse in an inducible Gorab^{Prx1} mouse model with the *Gorab* gene being deleted in mice at ten weeks of age. We hypothesized that tamoxifen-treated *Gorab* inducible knockout mice, with an intact OLCN will show a comparable mechanoresponse to that of the vehicle-treated mice. We aimed to gain a better understanding of the OCLN's role in mechanotransduction in GO patients.

Study 2 – The effect of rearing housing system on the keel density and microstructure in egg-laying hens

The goal of this study was to assess whether rearing housing style influences keel bone microstructure and density. We aimed to compare the keel bone microstructural parameters of hens reared in conventional cages to that of hens reared in high complexity aviaries. Moreover, this study aimed to determine whether hens with keel bone fractures have deleterious alterations to the keel bone microstructure and density, compared to those with intact keels. We hypothesized that hens reared in high complexity aviaries would show greater microstructural keel bone parameters. We also hypothesized that non-fractured keel bones would show superior cortical bone outcomes than fractured keel bones.

Chapter 2

Mechano-adaptation in *Gorab* inducible knockout mice

2.1 Preface

Gerodermia osteodysplastica (GO) is a hereditary segmental progeroid disorder caused by the loss of function mutation in the *GORAB* gene. GO individuals suffer from high incidents of bone fractures and shows pronounced osteoporosis at a very young age [111]–[114]. Previous studies revealed that GORAB is localized to the Golgi apparatus in dermal fibroblasts and osteoblasts, the cell types most likely affected in GO [113], [115]. Furthermore, this study reported that GORAB is mainly localized in the trans-Golgi, which is the major secretory pathway sorting station [115].

These studies also support that GORAB can be classified as a golgin [2]. Since golgins are involved in vesicle trafficking, GORAB might influence protein interaction and distribution. A study investigated this, and revealed that GORAB promotes COPI recruitment, which is an important mediator of protein trafficking [116]. So, it is evident that GORAB mutations impair

COPI retrieval and caused a deficit in glycosylation of secretory cargo proteins [116]. Data from an animal study also showed reduced proteoglycan glycanation in skin and bone tissue, which led to altered proteoglycans, overactivation of TGF-β and enhanced downstream signaling in the bone tissue of conditionally inactivated *Gorab* mice [117]. Consequently, GO can be regarded as a congenital disorder of glycosylation (CDG), characterized by a disorganized collagen matrix [117]. The loss of GORAB in the Golgi compartment also perturbs pre-osteoblasts, causing osteoblast dysfunction and low bone turnover kinetics, which is in contrast to another progeroid disorder, osteogenesis imperfecta [117].

Previously our collaborator, Dr. Uwe Kornak, developed a mouse model of Gorabfl/fl;Prx1creER ($Gorab^{Prx1}$) wherein the *Gorab* gene was conditionally knocked-out in the long bones from conception [117], [118]. These $Gorab^{Prx1}$ mice showed phenotypic characteristics similar to GO, including growth retardation, reduce cortical and trabecular bone volume, and increased osteocyte lacunar density [117], [118]. We also observed an increased anterior convexity in the tibiae of these mice, associated with reduced whole-bone strength and stiffness of $Gorab^{Prx1}$ mice compared to littermate controls (LC). Given that this nano-scale organization is formed by the interconnection of osteocytes and is thought to be responsible for the flow of interstitial fluid to produce osteocyte mechanical stimulation, the increased lacunar density observed in biopsies of GO donors and in the $Gorab^{Prx1}$ mouse model [117], may have a direct effect on the mechanoresponse of GORAB deficient bone. Therefore, our research group performed two weeks of daily tibial loading on 10-week-old female $Gorab^{Prx1}$ mice and showed that their bone formation response to loading was significantly impaired [110]. Further, studies by our group in collaboration with Dr. Richard Weinkamer showed that these mice had abnormal osteocyte morphology and a reduced and disrupted osteocyte lacunocanalicular network (OLCN) [119]. Together these data suggested that further investigation is needed to determine if the reduced mechanoresponse seen in these $Gorab^{Prx1}$ mice is due to the altered OLCN or due to the absence of the *Gorab* gene.

2.2 Introduction

Gerodermia osteodysplastica (GO) is a segmental progeroid disorder caused by loss-of-function mutations in the *GORAB* gene, associated with early onset osteoporosis and bone fragility [111]–[114]. As described in the Preface, we previously observed that *Gorab* conditional knockout mice ($Gorab^{Prx1}$) have a reduced mechanoresponse and a disrupted osteocyte lacunocanalicular network (OLCN) compared to littermates [110], [119].

As described in chapter 1, osteocytes function as the regulator of osteoblast and osteoclast activity, which in return regulates bone (re)modelling to maintain optimum bone mass. Furthermore, osteocytes interconnect to form the OLCN which is believed to sense mechanical strain through their intricate network of cell bodies inside fluid-filled lacunae [29]. Under mechanical strain conditions, the interstitial fluid flow can deform the osteocytes and the fluid shear stress can cause osteocytes to produce soluble factors that regulate osteoblast and osteoclast activity [120]–[122]. The anisotropy and alignment of fibular osteocytes (relatively elongated and aligned to the local mechanical loading conditions) suggest that osteocytes can directly sense matrix strain due to external loading of bone [123]. It is unknown how this mechanosensing signaling pathway is affected by the abnormal osteocyte morphology seen in our previous Gorab study [117]. Studies have shown that disease and aging can cause variations in osteocyte morphology and OLCN architecture, which results in changes in the osteocyte signaling pathway and mechanoresponse [35], [124]–[126], [102]. These studies suggests that bone mechanoresponse is affected by disorganized OLCNs, therefore both the OLCN architecture and the local mechanical strain should be considered in predicting bone mechanoresponse.

In the $Gorab^{Prx1}$ mice, the loss-of-function mutation is already present during crucial developmental stages, which likely caused these mice to develop altered OLCNs. Although our previous study showed that 10-week-old female $Gorab^{Prx1}$ mice had an impaired bone formation response to mechanical loading [110], it could not be ascertained whether the loss in mechano-adaptation was due to the altered OLCN or loss of the *Gorab* gene. Therefore, further studies are needed, using inducible Cre-models.

Inducible Cre models are very useful because Cre expression can be induced at a specific time and in a specific tissue, which is an ideal model for this study. Tamoxifen treatment can be used to induce Cre, although the doses of the inducer agent must be carefully optimized to avoid “leaky” expression of the gene and to avoid altering bone formation and resorption [4]. Another way to account for any “leaky” expression of the Cre recombinase, is to include controls with an identical genotype, ideally littermate controls, who are treated with vehicle instead of tamoxifen [4]. Caution must be taken when using these inducible Cre models as each model has its own limitations and vary in efficiency.

The aim of this study was to determine if the reduced mechanoresponse was primarily due to the loss of *Gorab* in osteocytes or a consequence of the developmentally altered OCLN. We compared the mechanoresponse in an inducible Gorab mouse model of *Gorab* with data previously obtained from the conditional Gorab^{Prx1} mouse model [110]. We hypothesized that tamoxifen-treated *Gorab* inducible knockout mice, with an intact OLCN will show a comparable mechanoresponse to that of the vehicle-treated mice. Results from this work may enable us to gain a better understanding of the OCLN’s role in mechanotransduction in GO patients.

2.3 Materials and Methods

2.3.1 Mouse model

The CAGGCre-ER mouse model for this study was developed by crossing CAGGCre-ER mice with Gorab$^{Flox/Flox}$ mice. The Cre-estrogen-receptor expression is controlled by the chicken beta actin promoter and is expressed in all cells. This Cre-estrogen-receptor fusion protein is slightly modified so that it is only activated by tamoxifen. At the desired age, mice are injected with tamoxifen, called the tamoxifen-treated group, which activates the Cre-estrogen-receptor fusion protein to translocate to the nucleus and mediate recombination of loxP sites flanking the *Gorab* gene. This ensures that the *Gorab* gene is present during the mouse's developmental stages of life and is only inactivated right before the experiment is conducted. All procedures were approved by the Canadian Council for Animal Care and the McGill University animal care committee (2016-7821).

2.3.2 Tamoxifen treatment

Fifteen, eight-week-old, female Gorab inducible knockout (iKO) mice were received from Charité - Universitätsmedizin Berlin, Germany, and housed in the animal facility at McGill University Health Center, Montreal, Canada. The mice were in quarantine for two weeks, acclimatized and randomized into two groups: 1) tamoxifen-(tamox) and 2) vehicle (vehicle) treated. All animals were housed in the same type of cages, five mice per cage, tamoxifen- and vehicle-treated mice in separate cages, with equal access to food and water. At ten-weeks of age, the tamoxifen-treated group received three intraperitoneal tamoxifen injections, 10 mg/kg every second day, while the vehicle-treated group received vehicle injections (corn oil: ethanol in a 9 to 1 ratio, volume: 10 mg/kg). A week was allowed for tamoxifen excretion.

2.3.3 In-vivo loading experiment

After the injection of tamoxifen (n=7) or vehicle (n=7), two weeks of in vivo cyclic compressive loading was applied to the left tibia of 12-week-old Gorab iKO mice.

The mechanical load was applied by an in vivo loading machine (Testbench, ElectroForce, LM1, Bose, Framingham, USA) that consist of an electromagnetic actuator and a load cell. With the limb (tibia) placed horizontally in between the actuator and load cell, the actuator applies a compressive load on the limb while the load cell measures the transmitted load. The applied load induces tissue strain which is modulated by bone morphology and tissue material properties and plays a critical role in regulating bone growth and remodeling [127].

First, the mice were anesthetized with isofluorane (2% in 0.6 L/min O_2)then the left tibia was placed into the loading machine, with the left foot placed in the foot plate on the actuator. With the mouse leg bent, the knee fits into the knee cup on the load cell. A pre-load of -1.5 N was applied to ensure that the limb is secured in the machine. Previous studies established that an approximate strain level of + 1200 micro strain ($\mu\varepsilon$) elicit an osteogenic response in mouse tibia [127], [96]. Considering this, the daily loading cycle used for this study included 216 cycles, applied at 4 Hz, which delivered peak loads of – 11 N for vehicle mice and -5.4 N for tamox mice. The right limb acted as the non-loaded internal control. It is the convention in the field to use the non-loaded control limb rather than additional sham loaded mice, since in vivo tibial loading is known to only have local rather than systemic effects [128], [48]. Normal cage activity was allowed between loading sessions.

2.3.4 In vivo micro-computed tomography (μCT) imaging

To evaluate the mechanoresponse of these tamoxifen- and vehicle-treated groups, in vivo μCT (SkyScan 1276, Bruker) was used to scan both the left and right tibiae of these mice after the in vivo loading experiment was conducted. The high-resolution μCT scanner at the Shriners Hospital for Children (Montreal, Canada), allowed us to quantify how the density and microstructural parameters changed in response to loading. Similar to the previous Gorab^{Prx1} study, we chose day 0, 5, 10 and 15 of the loading experiment as time points on which the

mice were scanned. On these days, the mice were loaded first, the scanner was switched on for its warm-up period (approximately 15 minutes), the mice were anesthetized with isofluorane (2% in 0.6 L/min O_2) and placed into the in vivo µCT. For the duration of the scan (approximately 20 minutes) the mice were anesthetized, monitored, and accumulated radiation dose was estimated to 150 mGy per scan. Before and during scanning, the mice were monitored in accordance with McGill SOP 110. The first scan (day 0) was used as the baseline scan and the same scanning procedure was repeated on day 5, 10 and 15. The scanning parameters was set to: 8 µm voxel size, 70 kV, 57 µA, 0.5 mm Al filter, 0.3° rotation and 180° scanning. Each day, after the last scan, phantoms were scanned at the same scanning settings and used for calibration of the volumetric bone mineral density measurements. After the final scan on day 15, the anesthetized mice were euthanized by carbon dioxide inhalation, the tibiae with the fibulae intact were dissected and stored in 100% ethanol.

2.3.5 Micro-computed tomography (µCT) analysis of the cortical mid-diaphysis

Bruker XRM solutions include all software needed to reconstruct scans from 2D projection images into 3D volumes (NRECON) and to conduct 2D and 3D analyze (CTAN) of the bone microstructure. The volume of interest (VOI) used to calculate the cortical bone microstructural parameters was selected as 5% of the tibial length at the midshaft of the tibia. Since the scan resolution was 8 µm the total tibial length was calculated by multiplying the number of scan slices by 0.008. The mid-slice was calculated and the VOI was centered around the mid-slice, therefore 2.5% of the tibial length was calculated and measured above and below the mid-slice. Once the VOI was cropped for each scan, a global threshold value of 0.98 mgHA/cm^3 was chosen as 120% of the OTSU threshold to segment cortical bone from soft tissue. 2D and 3D analysis were completed with CTAN and included parameters such as: cortical thickness (Ct.Th.), cortical area (Ct.Ar.), total cross-sectional area inside the periosteal envelope (Tt.Ar), cortical area fraction (Ct.Ar./Tt.Ar.), marrow area (Ma.Ar), cortical volumetric tissue mineral density (Ct.vTMD) and principal moments of inertia (Imax, Imin).

2.3.6 Histomorphometry

Each mouse received an intraperitoneal calcein injection (25 mg/kg) at 12 and 3 days before euthanasia. These intraperitoneal injections were done while the mice were still under anesthesia from the loading. After the two-week loading experiment and μCT imaging, the mice were euthanized, dissected, and the tibiae embedded in polymethyl methacrylate (PMMA).

The embedded bone samples were sectioned at the midshaft, in the transverse plane, with a high-speed band saw (IsoMet Low Speed Precision Cutter, Buehler, USA). After the surface of the samples were polished and buffed, the cross-section area of each tibia was imaged with a confocal laser scanning microscope (Zeiss LSM780, McGill University Health Center, Montreal, Canada) at 20x magnification.

Bioquant Osteo (BIOQUANT Image Analysis Corporation, Nashville, TN) software was used to analyze the confocal microscope images for cortical single and double-labeled surfaces, mineral apposition rate, mineralizing surface per bone surface and bone-formation rate per bone surface.

2.3.7 Gene expression analysis

For this study, it is important to confirm whether mRNA or protein expression levels of GORAB has been inactivated in the targeted tissues, the long bones. The level of *Gorab* knockout achieved in the study was determined by extracting RNA from the mice's flash frozen femur cortices (both tamox and vehicle group). These femur cortices were crushed with a mortar and pestle until the bone was a fine powder. RNA was isolated with Aurum total RNA mini-Kit (BioRad). Nanodrop was used to measure RNA concentration before qPCR was performed with QuantStudio 7. Averaged GAPDH and Hprt were used as reference genes and relative *Gorab* expression was calculated using the ΔCt method. The TaqMan probes GAPDH (Mm99999915_g1), Hprt (Mm03024075_m1) and Gorab (Mm00724788_m1) were used.

2.3.8 Statistical analysis

μCT data was analyzed at day 0, day 15 and as the change from baseline (day 15 - day 0) using a repeated measure ANOVA (SAS 9.4, Cary, USA) to examine the effect of treatment (tamox vs vehicle) and loading (control vs loaded). Paired t-tests were performed to compare genotype. Tukey Post-Hoc tests were performed to compare tamox to vehicle mice. A p value < 0.05 was considered significant. All results reported were significant, unless otherwise indicated. A p value $0.05 > p < 0.1$ was considered a trend. Note: p values were not adjusted for multiple comparisons.

2.4 Results

2.4.1 Loading led to a robust mechanoresponse

At day 0, ANOVA showed that loading had no effect on any diaphyseal cortical parameters. This indicates that there was no handedness (differences between right and left tibiae). The ANOVA showed that there was no significant effect of genotype on the density or any of the microstructural parameters, except Ma.Ar. A Tukey-Kramer post-hoc test revealed that Ma.Ar was significantly different between the control limbs of tamoxifen- and vehicle-treated groups on day 0.

On day 15, ANOVA showed that loading had a significant effect on Imin, Imax, Ct.Ar, Tt.Ar, Ct.Ar/Tt.Ar, and Ct.Th. Paired t-test showed significantly greater Imin (20%), Imax (29%), Ct.Ar (7%), and Ct.Th (8%) in the loaded limb compared to the non-loaded control limb of tamox mice. In the vehicle mice, paired t-test showed significantly greater Imax (13%), Ct.Ar (8%), Tt.Ar (2%), Ct.Ar/Tt.Ar (5%), and Ct.Th (9%) in the loaded limb compared to the non-loaded control limb.(See table 1 for mean ± SD values.)

Day 15 - 0, ANOVA showed similar effects as in the absolute values observed at day 15. Loading had a significant effect on Imin, Imax, Ct.Ar, Tt.Ar, Ct.Ar/Tt.Ar, and Ct.Th. Paired t-test for measures reported as a change from baseline (day 15 – 0) showed significantly greater Imin, Imax, Ct.Ar, Tt.Ar and Ct.Th in the loaded limb compared to the non-loaded control limb of tamox mice. In the vehicle mice, paired t-test showed significantly greater Imin, Imax, Ct.Ar, and Tt.Ar in the loaded limb compared to the non-loaded control limb. (See Fig.2 for illustration of μCT results as a change from baseline (day 15 – 0) and compared to μCT results of the previous study.)

2.4.2 Tamoxifen- and vehicle-treated mice had a similar mechano-adaptive response

On day 15, ANOVA showed that treatment had a significant effect on Ct.Ar/Tt.Ar and Ma.Ar. The Ct.Ar/Tt.Ar was greater in the tamox group than the vehicle group, while the Ma.Ar was greater in the vehicle group than the tamox group (table 1). However, when analyzing the difference (day 15 - 0), ANOVA showed that treatment did not have an effect on any of the cortical parameters.

For both measures reported at day 15 and as a change from baseline (day 15 – 0), ANOVA showed that there was no significant interaction between treatment groups and loading. This indicates that the tamoxifen-treated group had a similar response to loading to that of the vehicle-treated group for all cortical parameters measured (Fig. 2).

2.4.3 *Gorab* expression still present after tamoxifen treatment

Our qPCR results revealed a *Gorab* knockout level of only 10% in femurs of the inducible knockout mice.

No histomorphometry data was analyzed since the study was terminated prematurely (see Discussion section for details).

2.5 Discussion

The aim of our study was to determine if the reduced mechanoresponse was primarily due to the loss of *Gorab* in osteocytes or a consequence of the developmentally altered OCLN. We measured a similar mechano-adaptive response after two weeks of in vivo tibial loading in tamoxifen-treated and vehicle-treated mice. However, since the RNA can only be extracted from the femurs of these tamoxifen-treated mice after completion of the experiment and µCT-imaging, it was not possible to determine the level of *Gorab* expression in the mice long bones before the start of the experiment. Preliminary studies carried out by our collaborators, suggested a 50% knockout in tamoxifen-treated mice with our tamoxifen protocol. However, after the experiment, our qPCR results revealed a much lower knockout level of only 10%. Once this finding was revealed all further analyses, including trabecular bone analysis and histomorphometry were stopped and the study was terminated.

2.5.1 Appropriate tamoxifen dosage necessary for successful knockout

The tamoxifen injection dose used in our protocol (10 mg/kg every second day) is lower than commonly used concentrations (50-100 mg/kg) because a higher dosage may impact the bone microstructure [129]. So, since we investigated the bone microstructure of these mice, we chose a lower tamoxifen dose, which seemed to have been unsuccessful. We have since imported more Gorab mice from our collaborators at the Charite and commenced breeding. We are currently conducting a pilot study to examine the effectiveness of different doses of tamoxifen. We have two groups of CreERT Prx-Cre; Gorab fl/fl mice that received 3 injections of tamoxifen (Sigma T56480), on Monday, Wednesday, and Friday at 9-weeks-of-age. Group one received 10 mg/kg while group two received 20 mg/kg of tamoxifen per injection. One week was allowed for tamoxifen excretion, followed by two weeks of in vivo

loading at the same settings as in our previous study. This first batch of the pilot study, including littermate controls, was euthanized and the tibiae and femurs dissected on September 6th, 2021. In the meantime, breeding is underway to fill up these groups and once the pilot study is completed another student in our lab will repeat the study. A more recent study also showed that low doses may also impact bone microstructure. Untreated groups might need to be added to investigate this effect [130].

2.5.2 How vehicle-treated iKO mice compare to Gorab^{Prx1} littermates

We further investigated factors that might have influenced the tamoxifen treatment in our mice, by comparing our vehicle-treated mice to the littermates of the previous Gorab^{Prx1} study. For both studies, colonies were received from our collaborators in Berlin, although the previous stud was conducted in 2015 while our study was conducted in 2020. This time difference may have caused potential drift in colonies.

In both these studies, female C57BL/6 mice underwent two weeks of loading and were µCT-imaged on day 0, 5, 10, and 15 [131]. The in vivo loading was performed by the same loading machine with the same loading settings for both studies, although, in the iKO study the mice were scanned with a Bruker SkyScan 1276 while a Scanco VivaCT 40 was used to scan the Gorab^{Prx1} mice [131]. There was a recent study that showed some trabecular bone parameters were calculated differently based on analysis software used [132]. Also, while the iKO study used a scanning resolution of 8 µm, the Gorab^{Prx1} study scanned mice at 10.5 µm. These differences in scanner and scan resolution might account for variations in the bone microstructural parameters between these groups. At baseline, our iKO vehicle-treated mice showed greater Imax, Ct.Ar, Tt.Ar, Ct.Th and Ct.vTMD than the Gorab^{Prx1} LC of the previous study. Although statistical analysis was not performed, both groups showed a similar response to loading, which indicates that this data is comparable.

2.6 Conclusions

We have previously observed an altered OLCN and reduced mechanoresponse in the Gorab^{Prx1} mice. The current study using tamoxifen-treated mice was inconclusive since the knockout of the gene was insufficient. Once appropriate knockout of the gene is possible by optimization of tamoxifen protocols, future studies are necessary to determine if the loss of mechanoresponse in *Gorab* deficient mice is due to deterioration of the OLCN or deletion of the gene. These data could lead to novel therapeutic targets to address low bone mass in GO since bone biopsies from patients also showed disorganized OLCNs.

2.7 Figures and tables

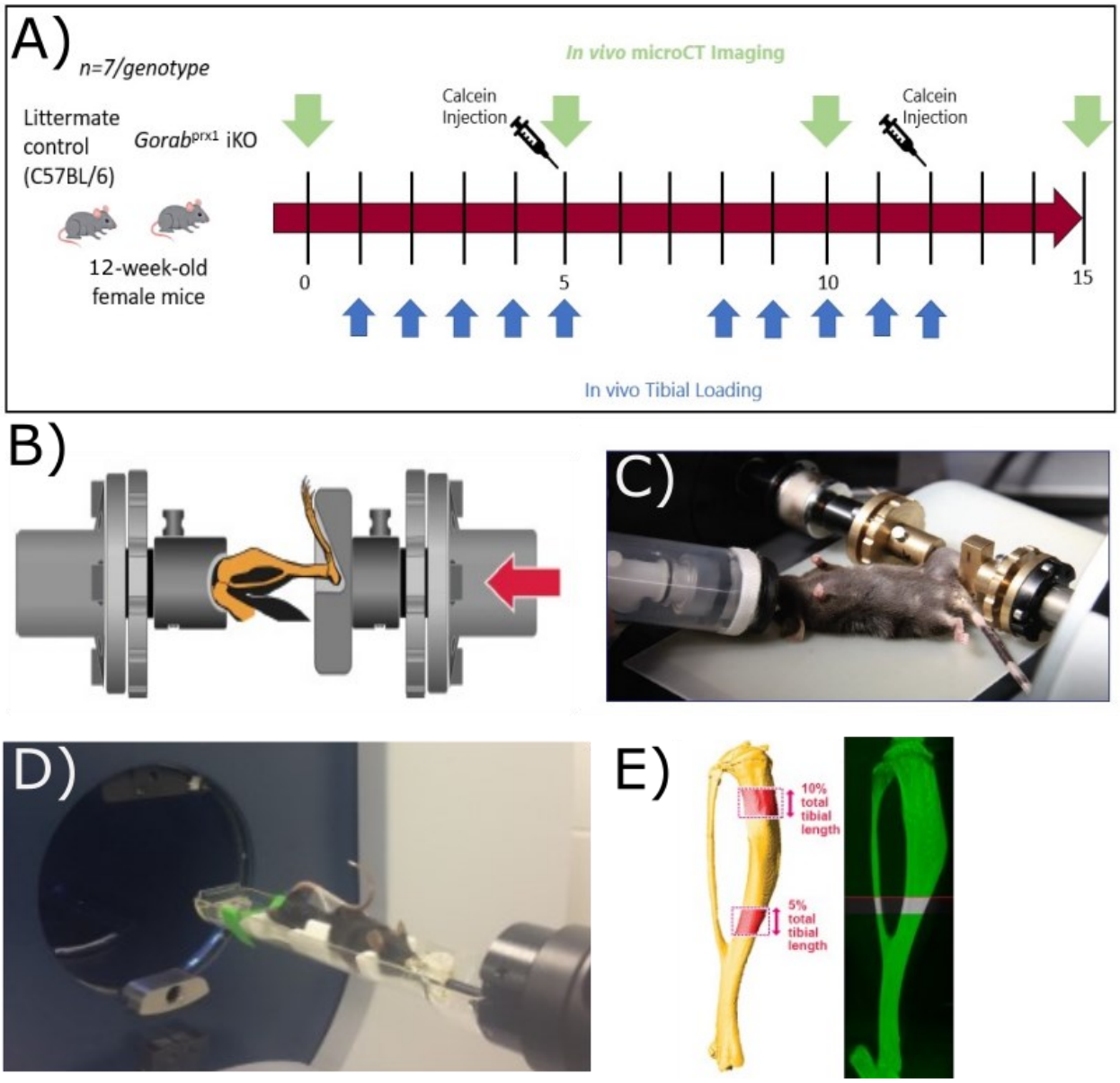

Figure 1: Experimental design; A) Experiment timeline of the two-week in vivo loading experiment (blue arrows), the in vivo microCT imaging on day 0, 5, 10, 15, and the injection of calcein 3 and 10 days prior to euthanasia. B) Schematic of in-vivo tibial loading, C) loading experiment set-up of the left limb placed within the loading machine, D) µCT scanning set-up of the anesthetized mouse in the scanner cassette, E) location of diaphysis volume of interest within the tibia.

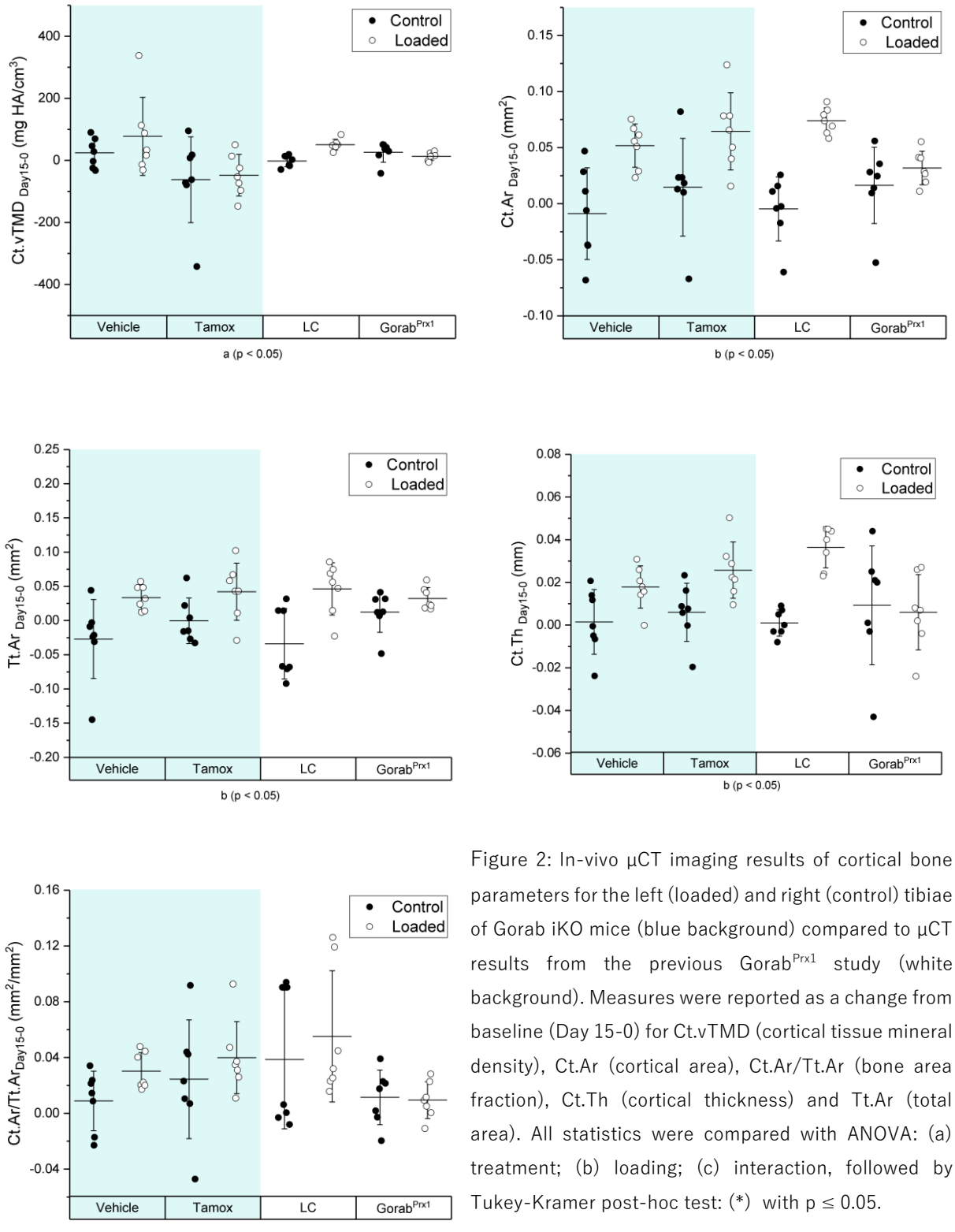

Figure 2: In-vivo µCT imaging results of cortical bone parameters for the left (loaded) and right (control) tibiae of Gorab iKO mice (blue background) compared to µCT results from the previous Gorab^{Prx1} study (white background). Measures were reported as a change from baseline (Day 15-0) for Ct.vTMD (cortical tissue mineral density), Ct.Ar (cortical area), Ct.Ar/Tt.Ar (bone area fraction), Ct.Th (cortical thickness) and Tt.Ar (total area). All statistics were compared with ANOVA: (a) treatment; (b) loading; (c) interaction, followed by Tukey-Kramer post-hoc test: (*) with $p \leq 0.05$.

Table 1 In-vivo µCT imaging results of cortical bone parameters for the left (loaded) and right (control) tibiae of Gorab iKO tamoxifen-treated (tamox) and vehicle-treated (vehicle) mice at two scanning time points (Day 0, 15). Data presented as mean ± standard deviation. All statistics were compared with ANOVA: (a) treatment; (b) loading; (c) interaction, followed by Tukey-Kramer post-hoc test: (*) with $p \leq 0.05$.

	Tamox		Vehicle	
	control	loaded	control	loaded
Day 0	(n=7)	(n=7)	(n=7)	(n=7)
Imax(mm^4)	0.08 ± 0.02	0.08 ± 0.02	0.08 ± 0.02	0.08 ± 0.01
Imin (mm^4)	0.05 ± 0.01	0.05 ± 0.01	0.05 ± 0.01	0.05 ± 0.01
Ct.Ar (mm^2)	0.59 ± 0.07	0.59 ± 0.07	0.60 ± 0.06	0.59 ± 0.06
Tt.Ar (mm^2)	0.92 ± 0.09	0.93 ± 0.11	0.99 ± 0.06	0.96 ± 0.08
Ct.Th (mm)	0.23 ± 0.02	0.23 ± 0.02	0.23 ± 0.01	0.23 ± 0.02
Ma.Ar (mm^2) a*	0.34 ± 0.03	0.34 ± 0.04	0.38 ± 0.02	0.37 ± 0.03
Ct.Ar/Tt.Ar (mm^2/ mm^2)	0.64 ± 0.02	0.64 ± 0.03	0.61 ± 0.03	0.62 ± 0.02
Ct.vTMD (mg HA/cm^3)	1500 ± 139	1538 ± 150	1441 ± 123	1470 ± 108
Day 15	(n=7)	(n=7)	(n=7)	(n=7)
Imax(mm^4)b	0.07 ± 0.02	0.09 ± 0.02	0.08 ± 0.01	0.09 ± 0.02
Imin (mm^4)b	0.05 ± 0.01	0.06 ± 0.01	0.05 ± 0.01	0.06 ± 0.01
Ct.Ar (mm^2)b	0.61 ± 0.07	0.65 ± 0.06	0.59 ± 0.04	0.64 ± 0.07
Tt.Ar (mm^2)b	0.93 ± 0.09	0.97 ± 0.1	0.96 ± 0.05	0.99 ± 0.08
Ct.Th (mm)b	0.24 ± 0.01	0.26 ± 0.01	0.23 ± 0.01	0.25 ± 0.02
Ma.Ar (mm^2) a*	0.32 ± 0.04	0.32 ± 0.05	0.36 ± 0.02	0.35 ± 0.02
Ct.Ar/Tt.Ar (mm^2/ mm^2)	0.66 ± 0.03	0.68 ± 0.02	0.62 ± 0.01	0.65 ± 0.03
Ct.vTMD (mg HA/cm^3)	1438 ± 58	1490 ± 112	1466 ± 136	1547 ± 168

2.8 Supplementary Information

Supplementary table 1: Previously reported µCT parameters of cortical bone mass and microstructure at two scanning time points (Day 0, 15) in left (loaded) and right (control) limbs of Gorab^{Prx1} and littermate control (LC) mice. Data presented as mean ± standard deviation. All statistics were compared with ANOVA: (a) genotype; (b) loading; (c) interaction, followed by Tukey-Kramer post-hoc test: (*) with $p \leq 0.05$.

	Gorab^{Prx1}		LC	
	control	loaded	control	loaded
Day 0	(n=6)	(n=6)	(n=6)	(n=6)
Imax(mm^4)	0.04 ± 0.01	0.03 ± 0.01	0.06 ± 0.01	0.06 ± 0.01
Imin (mm^4)	0.03 ± 0.01	0.03 ± 0.01	0.05 ± 0.01	0.05 ± 0.01
Ct.Ar (mm^2)	0.41 ± 0.08	0.39 ± 0.07	0.55 ± 0.04	0.54 ± 0.04
Tt.Ar (mm^2)	0.49 ± 0.08	0.48 ± 0.08	0.68 ± 0.06	0.69 ± 0.05
Ct.Th (mm)	0.17 ± 0.04	0.16 ± 0.04	0.20 ± 0.01	0.19 ± 0.01
Ct.Ar/Tt.Ar (mm^2/ mm^2)	0.83 ± 0.06	0.82 ± 0.07	0.81 ± 0.03	0.79 ± 0.01
Ct.vTMD (mg HA/cm^3)	1241 ± 54	1228 ± 58	1293 ± 13	1258 ± 22
Day 15	(n=6)	(n=6)	(n=6)	(n=6)
Imax(mm^4)$_b$	0.04 ± 0.01	0.04 ± 0.01	0.06 ± 0.01	0.07 ± 0.01
Imin (mm^4)$_b$	0.03 ± 0.01	0.03 ± 0.01	0.04 ± 0.01	0.05 ± 0.01
Ct.Ar (mm^2)$_b$	0.44 ± 0.06	0.44 ± 0.06	0.55 ± 0.04	0.61 ± 0.03
Tt.Ar (mm^2)$_b$	0.52 ± 0.06	0.52 ± 0.08	0.65 ± 0.07	0.73 ± 0.06
Ct.Th (mm)$_b$	0.18 ± 0.03	0.18 ± 0.02	0.20 ± 0.02	0.23 ± 0.01
Ct.Ar/Tt.Ar (mm^2/ mm^2)	0.85 ± 0.05	0.85 ± 0.04	0.85 ± 0.04	0.84 ± 0.04
Ct.vTMD (mg HA/cm^3)	1268 ± 30	1254 ± 20	1294 ± 19	1310 ± 18

Supplementary table 2: µCT parameters of cortical bone mass and microstructure at two scanning time points (Day 0, 15) in left (loaded) and right (control) limbs of Gorab iKO littermate control mice compared to $Gorab^{Prx1}$ littermate control (LC) mice. Data presented as mean ± standard deviation.

	iKO vehicle-treated		$Gorab^{Prx1}$ LC	
	control	loaded	control	loaded
Day 0	(n=7)	(n=7)	(n=6)	(n=6)
Imax(mm^4)	0.08 ± 0.02	0.08 ± 0.01	0.06 ± 0.01	0.06 ± 0.01
Imin (mm^4)	0.05 ± 0.01	0.05 ± 0.01	0.05 ± 0.01	0.05 ± 0.01
Ct.Ar (mm^2)	0.60 ± 0.06	0.59 ± 0.06	0.55 ± 0.04	0.54 ± 0.04
Tt.Ar (mm^2)	0.99 ± 0.06	0.96 ± 0.08	0.68 ± 0.06	0.69 ± 0.05
Ct.Th (mm)	0.23 ± 0.01	0.23 ± 0.02	0.20 ± 0.01	0.19 ± 0.01
Ct.Ar/Tt.Ar (mm^2/ mm^2)	0.61 ± 0.03	0.62 ± 0.02	0.81 ± 0.03	0.79 ± 0.01
Ct.vTMD (mg HA/cm^3)	1441 ± 123	1470 ± 108	1293 ± 13	1258 ± 22
Day 15	(n=7)	(n=7)	(n=6)	(n=6)
Imax(mm^4)	0.08 ± 0.01	0.09 ± 0.02	0.06 ± 0.01	0.07 ± 0.01
Imin (mm^4)	0.05 ± 0.01	0.06 ± 0.01	0.04 ± 0.01	0.05 ± 0.01
Ct.Ar (mm^2)	0.59 ± 0.04	0.64 ± 0.07	0.55 ± 0.04	0.61 ± 0.03
Tt.Ar (mm^2)	0.96 ± 0.05	0.99 ± 0.08	0.65 ± 0.07	0.73 ± 0.06
Ct.Th (mm)	0.23 ± 0.01	0.25 ± 0.02	0.20 ± 0.02	0.23 ± 0.01
Ct.Ar/Tt.Ar (mm^2/ mm^2)	0.62 ± 0.01	0.65 ± 0.03	0.85 ± 0.04	0.84 ± 0.04
Ct.vTMD (mg HA/cm^3)	1466 ± 136	1547 ± 168	1294 ± 19	1310 ± 18

Chapter 3

The effect of rearing housing system on the keel density and microstructure in egg-laying hens

3.1 Introduction

In Canada, a total of 26 million hens produces about 7.2 billion eggs per year [133]. The White Leghorns and Rhode Island Red are the main breeds of laying hens, with Lohmann White being the most common breed [133]. Compared to traditional breeds, commercial strains are genetically selected for increased egg laying, with the onset of lay from 16 to 18 weeks of age. On average, hens produce one egg per day, a rate considerably higher than the natural rate of laying. Therefore, commercial farms prefer housing systems that allow for easy collection of eggs. Commonly, these housing systems are conventional cages or

furnished cages with restricted opportunities for natural behavior and activities. As a result, these commercial strains show greater loss of structural bone mass during lay than traditional breeds, which results in weakened bones [61].

A considerable welfare problem reported by commercial laying farms from several countries [22], [23], [24], [25] is that 70 to 97% of hens suffer from keel bone deformities at the end of lay. Since birds experience pain similar to that of mammals [134], recent research has been dedicated to address the high prevalence of keel bone damage and its effect on hen welfare in the egg-laying industry. Besides being associated with pain, keel bone fractures also lead to decreased egg production [135] and increased mortality [136], which have a detrimental economical effect [137]. The Canadian Poultry Association has announced that the poultry industry will be moving towards aviary housing systems completely by 2023 in an attempt to provide a more enriched environment and one that allows chickens more opportunity for physical activity.

In avian species, the keel bone is an extension of the sternum and serves as an anchor for flight muscles: pectoralis major and pectoralis minor (Fig. 4A) [138], [139]. These muscles are used for wing flapping, during which the pectoralis muscles undergo proportionally large length changes (muscle strain) [140]. This muscle strain exerts a mechanical load on the keel bone [40], [41]. Although the growth of long bones ceases at the onset of lay (16 to 18 weeks of age) [141], [142], keel bone ossification is slower and continues until approximately 28 to 40 weeks of age [143], [144], [145]. Because the keel growth and ossification begin in the cranial region of the keel and progresses to the caudal tip, the caudal tip of the keel is still cartilaginous during the first couple of weeks of lay [63]. Previous studies have reported that keel-bone damage usually occurs along the spine and caudal tip, independent of the housing system during lay, and that fracture incidences increase with age [146], [22], [147], [148]. So, even after the caudal tip is completely ossified, keel fractures still occur during the laying phase, in both open non-cage systems (possibly due to high-impact crashes and falls [25], [149], [150] and conventional cages (the exact causes still unclear) [151], [152]. Surprisingly, a recent study reported that high energy collisions is not the main cause of keel fractures in aviary systems, since birds with keel fractures showed no markers associated with trauma [153]. So, if keel bone fractures still occur after keel bone ossification, and high-impact

collisions are not the main cause, it remains unclear what leads to increased fracture incidences with aging.

Studies have shown that bone biology in hens changes drastically at the onset of lay to accommodate for egg production [59], [154], [26]. This includes osteoblast activity shifting from cortical bone production to medullary bone production, which is the main source of calcium for eggshells. Meanwhile, osteoclast activity remains unchanged. As a result, hens show a reduction in bone mass, which leads to weaker bones that are more susceptible to fractures [26]. This decrease in bone mass continues until end of lay, which may explain why aging layers show increased fracture incidences.

Studies have reported that increased opportunity for physical activity during the rearing phase improves muscle growth and bone breaking strength in long bones, which was sustained until end of lay [155], [65]. One way to reduce fracture incidences in laying hens may be to develop pullets with higher bone mass, which results in stronger bones. Pullets exposed to increased opportunities for physical activity during rearing, may subject their bones to increased mechanical loading, stimulating increased bone apposition that can reduce bone fractures in later stages of life [143]. This way, these pullets can undergo bone reduction at the same rate during the laying phase, without their bones becoming critically weak and susceptible to fractures.

Therefore, the goal of this study was to assess whether rearing aviary style influences keel bone microstructure and density. Moreover, this study aimed to determine whether hens with keel bone fractures have deleterious alterations to the keel bone microstructure and density, compared to those with intact keels. This work focused on 30-week-old hens and is part of a larger study performed by other students who are looking at two additional age groups, namely 50 and 70 weeks of age.

3.2 Methods

All animal trials were carried out at the Arkell Poultry Research Station and performed according to Arkell Poultry Research Station Standard Operating Procedures (Arkell, ON, Canada).

3.2.1 Animal model

Two flocks of Lohmann Selected Leghorn Lite (white) and Lohmann Brown Lite (brown) birds were obtained from a commercial hatchery (Fig.4A). A total of 56 (n=6-7/genetic strain/housing/fracture status) pullets were sampled from consecutive flocks reared in conventional cages (CC) or high complexity aviaries (HCA). The HCA were balanced by genetic strain across the two flocks, whereas both genetic strains were reared in CC in each flock.

All birds had equal access to food and received a standard age-appropriate crumble diet ad lib. Each bird was assigned and labelled with a unique identification number such that all subsequent analyses were blinded to housing and genetic strain.

3.2.2 Housing

Pullets were reared in two types of housing systems, in conventional cages (Ford, Dickinson, Mitchel, Ontario, Canada) (Fig. 4C) or in high-complexity aviary systems (NivoVaria, Jansen Poultry Equipment, Netherlands and Farmer Automatic Portal Pullet Rearing System for Layers, Clark Ag System, Caledonia, Ontario, Canada) (Fig. 4B). Conventional cages (76 x 66 x 40 cm) were outfitted with two nipple drinkers and an external feeding trough. Chicks in these cages were brooded at a stocking density of 167 cm^2 / bird until three-weeks-of-age, after which they were evenly divided into 334 cm^2 / bird.

The two equivalent brands of high-complexity aviaries that were used, NivoVaria (726 x 236 x 265 cm) and Farmer (726 x 245 x 211 cm), were outfitted with two lines of nipple drinkers and feeding troughs, six perches, and a raised platform in the center of the system, all of which spanned along the length of the system. Until six-weeks-of-age, chicks were stocked at 128 cm^2/ bird (NivoVaria) and 138 cm^2 bird (Farmer) and had no access to the litter floor area, raised platforms or ramps. At six-weeks-of-age both systems were fully opened, the wall panels were rotated outwards, which created additional raised levels (127 cm^2 / bird in the NivoVaria and 104 cm^2 /bird in the Farmer) and access to the litter floor (75 cm^2 / bird in both systems) and ramps.

At 17-weeks-of-age all pullets were moved to furnished cages (Ford Dickinson Enriched Condo laying hen system, Mitchell, On, Canada) to begin their laying phase. In each cage (365 x 66 x 55 cm) pullets were stocked at 752 cm^2 / bird and had access to nipple drinkers, an external feeding trough, perches, a nest area (60 x 33 cm) and plastic scratch pad (60 x 33 cm). The number of pullets in each cage were reduced as pullets were euthanized for the project.

All housing systems were under the same light and temperature cycle during the first week of age (34 °C, $2h$ /$4h$ dark/light cycle at 40 lux), during rearing (incrementally lowered to 20 °C, $10h$ light/day and 10 lux)and kept at this light/temp cycle during the laying period.

3.2.3 Sample collection

At 30 weeks of age, birds from each genetic strain and housing system were randomly pre-selected by palpation for keel bone fractures. The keel bone of the pre-selected bird (pre-selected because the bird might not be placed into a sample group, depending on its fracture status) was radiographed to confirm fracture presence (Fig. 4D), and then a technician scored the degree of keel bone fracture [156] and grouped the bird as fractured (n =6-7) or non-fractured (n = 6-7).

The identification numbers of birds were documented, the birds were euthanized by carbon dioxide, weighed, refrigerated overnight and then frozen at – 20 °C. The carcasses were transported to the Shriners Hospital for Children in Montreal, Canada, where they were

thawed for 24 hours at room temperature before the keel bones (and other long bones and muscles) were excised, according to Casey-Trott et al.(2017a). Keel bones were wrapped in towels, soaked in 70% ethanol, double bagged (to avoid them from drying out), and stored at room temperature. Muscle samples from each bird were bagged and stored at -20°C.

3.2.4 Keel bone measurements

Before scanning, the keel bone was removed from its bag and placed on a white board with a ruler. The keel length was measured on the dorsal metasternum surface, with the cranial region parallel to the caudal tip. For the purpose of µCT analysis and determination of a volume of interest, the keel length was measured from the caudal tip to the carina apex (Fig.3) since these are visible landmarks that can easily be identified in all the keel bones.

Figure 3 Keel bone measurements

3.2.5 Micro-computed tomography (µCT)

Micro-computed tomography (µCT) was performed by the Bruker SkyScan 1276 at The Shriners Hospital for Children (Montreal, QC, Canada).

Prior to µCT, each keel bone was removed from its bag, cleaned to remove any soft tissue, photographed, measured, and placed in a Styrofoam splint (to protect the fragile keel tip during fixation of the keel bone in the scanner cassette) (Fig. 5B). The splinted keel bone was wrapped in its towel and replaced in its bag. The bone was then securely fixed in the

center of the scanner cassette with the tip of the keel at the distal end of the cassette. All bones were positioned and scanned in the same manner (Fig. 5C), with scanning parameters set as: 15 µm voxel size, 80 kV, 200 µA, 360° scanning, frame averaging of 2 and rotational step of 0.6°. Since limited studies have evaluated the keel microstructure, it was still undetermined what size volume of interest (VOI) would represent the entire keel microstructure. Therefore, we chose to scan the entire keel bone at a high resolution, resulting in a scanning time of 120 minutes per bone. For this study, birds housed in CC and HCA of both genetic strains, with fractures (n = 6-7) and without fractures (n = 6-7) were scanned. Each day, after the final scan of the day, phantoms of 0.25 and 0.75 mg HA/cm^3 density were scanned at the same scanning parameters. This was used to calibrate all the scans to units of mg HA/cm^3.

3.2.6 Selection of volume of interest

After µCT scanning, a representative volume of interest (VOI) was defined. The aim of the study was to evaluate intact bone microstructure of fractured and non-fractured keels, without including fracture sites within the VOI. Yet, we still wanted the VOI to be near common fracture sites since we compared fractured keel bone characteristics to that of non-fractured keel bones. Considering the size of the keel bone, a larger VOI of 20% of the keel length was chosen as an appropriate representative of the cortical and trabecular bone microstructure. Since most keel fractures occurred at the keel caudal tip, the VOI started at the mid-slice and included 20% of the keel length towards the caudal tip of the keel bone (Fig. 5A).

3.2.7 Micro-computed tomography (µCT) analysis of the cortical and trabecular bone

Bruker XRM solutions include all software needed to reconstruct scans from 2D projection images into 3D volumes (NRECON) and to conduct 2D and 3D analyze (CTAN) of the bone microstructure. Since the scan resolution was 15 µm, the total keel length was calculated by multiplying the number of slices in the scan by 0.015. The mid-slice and 20% of

the keel length were calculated and the VOI was cropped for each scan. To determine a global threshold, the histograms of a subset of 12 keel bone scans were analyzed. For each scan, we computed the OTSU threshold as well as variations of this value (80% OTSU, 90% OTSU, ….). Mean thresholds for each variation were computed from the subset, applied, and results visually inspected to select the optimal version. A global threshold value of 0.4385 mgHA/cm^3 was chosen (90% OTSU) to segment cortical bone from soft tissue. A global threshold value of 0.4488 mgHA/cm^3 was chosen (110% OTSU) to segment trabecular bone from soft tissue. 2D and 3D analysis were completed with CTAN to distinguish between cortical bone and trabecular bone. This was conducted in the same manner as in the mouse studied conducted by our lab, by characterizing the outer, denser layer of bone as cortical bone and the thinner, spongy-structured bone within the keel bone as trabecular bone.

cortical bone parameters such as: cortical thickness (Ct.Th.), cortical area (Ct.Ar.), total cross-sectional area inside the periosteal envelope (Tt.Ar), cortical area fraction (Ct.Ar./Tt.Ar.), marrow area (Ma.Ar), cortical volumetric tissue mineral density (Ct.vTMD), and principal moments of inertia (Imax, Imin). Trabecular bone parameters included: trabecular thickness (Tb.Th), trabecular number (Tb.N), trabecular separation (Tb.Sp), trabecular bone volume fraction (BV/TV) and trabecular volumetric tissue mineral density (Tb.vTMD).

3.2.8 Statistical analysis

µCT data was analyzed using a repeated measure ANOVA (SAS 9.4, Cary, USA) to examine the effect of genetic strain (brown vs white), housing (CC vs HCA) and fracture status (fracture vs non-fracture). An independent t-test was performed to compare housing, genetic strain, and fracture status. Tukey Post-Hoc tests were performed to compare genetic strain, housing, and fracture status. A p value < 0.05 was considered significant. All results reported were significant, unless otherwise indicated. A p value $0.05 > p < 0.1$ was considered a trend. Note: p values were not adjusted for multiple comparisons.

3.3 Results

3.3.1 Cortical microstructural outcomes were superior in conventional cages compared to high complexity aviary systems

ANOVA showed that housing style had a significant effect on these cortical bone parameters: Ct.vTMD, Ct.Ar, Ct.Ar/Tt.Ar, and Ct.Th. The Ct.vTMD was 8% greater in CC (mean ± standard deviation; 0.62 ± 0.08) than in HCA (0.57 ± 0.09); Ct.Ar was 14% greater in the CC (5.25 ± 1.02) than in the HCA (4.60 ± 1.30); Ct.Ar/Tt.Ar was 22% greater in the CC (0.30 ± 0.09) than in the HCA (0.25 ± 0.09); and Ct.Th was 15% greater in the CC (0.17 ± 0.03) than in the HCA (0.15 ± 0.03). (See Fig.6 for graphs and table 2 for mean ± SD values.)

T-tests showed significant differences in Ct.Ar between brown birds with fractures. In brown birds, fractured keel bones had greater Ct.Ar (22 %) in CC than in the HCA. T-test also showed significant differences in Ct.vTMD, Ct.Ar/Tt.Ar and Ct.Th in white birds with fractured. In the white birds, fractured keel bones showed greater Ct.vTMD (23%), Ct.Ar/Tt.Ar (50%), and Ct.Th (23%) in CC than in HCA.

3.3.2 Trabecular microstructural outcomes were superior in conventional cages compared to high complexity aviary systems

ANOVA showed that housing style had a significant effect on Tb.vTMD, Tb.BV/TV and Tb.Th. Tb.vTMD was 4% greater in the CC (0.57 ± 0.03) than in the HCA (0.55 ± 0.03); Tb.BV/TV was 58% greater in the CC (0.15 ± 0.11) than in the HCA (0.09 ± 0.09), and Tb.Th was 16% greater in the CC (0.08 ± 0.01) than in the HCA (0.07 ± 0.01). (See Fig.7 for graphs and table 3 for mean ± SD values.)

T-tests showed a trend in Tb.vTMD ($p = 0.069$), Tb.BV/TV ($p = 0.071$) and Tb.Th ($p = 0.081$) between brown birds with fractures. Brown birds in CC with fractures showed greater Tb.vTMD (5%), Tb.BV/TV (100%) and Tb.Th (3%) than brown birds in HCA with fractures.

3.3.3 Cortical and trabecular microstructural outcomes, and anthropometrics vary based on genetic strain

When analyzing the keel bone cortical parameters, ANOVA showed that genetic strain had a significant effect on Tt.Ar, Ma.Ar, Imin and Ct.Ar/Tt.Ar. The Tt.Ar was 38% greater in the brown (22.05 ± 3.70) than in the white (15.99 ± 3.34) birds, Ma.Ar was 50% greater in the brown (16.89 ± 3.81) than in the white (11.26 ± 3.72) birds, Imin was 88% greater in the brown (38.71 ± 12.03) than in the white (20.50 ± 7.73) birds, and Ct.Ar/Tt.Ar was 28% greater in white (0.31 ± 0.11) than in brown (0.24 ± 0.05) birds.

T-tests showed that genetic strain had a significant effect on the following cortical parameters: Brown bird in CC with fractures had greater Ct.Ar (18%), Tt.Ar (52%), Imin (107%), and Ma.Ar (68%) than white birds in CC with fractures. Brown bird in CC with no-fractures had greater Tt.Ar (38%) and Ma.Ar (59%) than white birds in CC with no-fractures. Brown birds in HCA with fractures showed greater Tt.Ar (36%), Imin (146%), Ma.Ar (40%), and Ct.Th (23%) than white birds in HCA with fractures. Brown birds in HCA with no-fractures showed greater Imin (58%) than white birds in HCA with no-fractures. (See section 3.7, table 2 for mean $\pm$SD values).

ANOVA also showed that genetic strain had a significant effect on Tb.Sp. The Tb.Sp was 31% greater in the brown (0.50 ± 0.25) than in the white (0.38 ± 0.16) birds.

When analyzing the body weight of the birds, ANOVA showed than genetic strain also had a significant effect on body weight. Body weight was 21% greater in the brown (2097 ± 218) than in the white (1737 ± 159) birds. (See table 4 for mean $\pm$SD values). The t-tests revealed that the brown birds in CC with fractures had significantly greater body weight (24%) than white birds in CC with fractures. Brown birds in CC with no fractures had significantly greater body weight (17%) than white birds in CC with no fractures. Brown birds in HCA with fractures had significantly greater body weight (26%) than white birds in HCA with fractures.

Brown birds in HCA with no fractures had significantly greater body weight (17%) than white birds in HCA with no fractures.

No significant difference was observed in keel length. For example, keel length of brown birds was 96.9 ± 8.6 while the keel length of white birds was 95.04 ± 3.7. (See table 4 for mean ± SD values).

3.3.4 Fractured keel bones had altered trabecular but similar cortical microstructural parameters to non-fractured bones

ANOVA showed that no significant differences were observed between the cortical parameters of fractured and non-fractured keel bones. For example, the mean and standard deviation (mean ± SD) Ct.Ar was 4.69 ± 1.15 in the fractured and 5.16 ± 1.2 in the non-fractured, and Ct.Th was 0.15 ± 0.03 in the fractured and 0.16 ± 0.03 in the non-fractured.

Interestingly, ANOVA showed than fracture status had a significant effect on Tb.Sp. The Tb.Sp was 42% greater in the fractured (0.52 ± 0.20) than in the non-fractured (0.36 ± 0.20) group.

3.4 Discussion

3.4.1 Do high complexity aviaries stimulate greater microstructural keel bone outcomes than conventional cages in 30-week-old hens?

In our study, surprisingly, most of the keel bone cortical and trabecular microstructural outcomes were superior in the conventional cages compared to the high complexity aviaries.

A previous study on the bone microstructure of 16-week-old Lohmann Selected Lite (white) laying hens reported that pullets reared in aviary rearing systems had greater cortical bone parameters than pullets reared in conventional cages for the radius, humerus and tibia [63]. Another study reported that microstructural characteristic of the tibiotarsus bone of 16-week-old pullets reared in aviary housing was enhances in Lohmann Selected Leghorn (LSL)-Lite birds compared to pullets reared in conventional caged housing [157]. Interestingly, the effect was genetic strain specific, in that they did not see a difference in microstructural properties in tibiotarsi from Lohmann Brown-Lite birds between aviary and conventional cage pullet rearing.

Our study also included Lohmann Selected Lite (white) and Lohmann Brown-Lite (brown) laying hens reared in conventional cages and high complexity aviaries, but we investigated the keel bone microstructure at 30-weeks-of-age. In contrary to these studies on the microstructure of pullet long bones, our results showed that white and brown birds reared in conventional cages had greater keel bone cortical parameters. We plan to analyze the microstructure of the radii, humeri, tibiae of our birds so that our study can be comparable to these previous studies. Only then can we make further conclusions about the effects of rearing housing system.

Casey-Trott et al. (2017a) did not measure keel bone microstructural outcomes. They only reported that the keel length, measured on the dorsal metasternum surface, parallel to the cranial region of the sternal notch, adjusted for body weight, was greater in the aviary systems compared to the conventional cages [63]. In our study, no significant differences were observed in the keel length between housing systems. When we adjusted keel length for body weight, as in Casey-Trott et al. (2017a), ANOVA showed that genetic strain had a significant effect, but housing style had no effect. This difference might be because of different keel bone lengths measured. We measured the ‘keel length’ from the caudal tip to the carina apex for the purpose of µCT analysis because the caudal tip and carina apex are prominent landmarks that are easily identified in all keel bones. To my knowledge, a standardized method of measuring the keel length is still to be determined.

Casey-Trott et al. (2017a) also measured the cartilage portion at the keel tip, that is not yet completely ossified, and reported that the keel bones of aviary-reared pullets had larger portions of cartilage compared to pullets reared in conventional cages. Whether this

cartilage portion is in proportion with the keel length or a potential indicator that ossification of the keel bone was slower in aviary-rearing, requires further investigation. We did not report any parameters on the cartilage portion of the keel tip in our study.

Furthermore, Erin Ross reported that aviary-reared Lohmann Brown Lite and Lohmann LSL-Lite pullets had stronger femora, radii, and humeri than birds reared in conventional cages [158]. Our study did not investigate the keel bone strength. E.Ross did not report keel bone lengths but calculated the keel bone area of these birds and reported that keel bones of birds reared in open-concept aviaries with maximum three-dimensional space, did not differ in proportional size from conventional cages or other aviary systems. In accordance with this study, Pufall et al. (2021) also showed no differences in pullet keel area between different aviary rearing systems [159]. Although we have not yet reported keel bone area, it may be useful to compare the area of the keel bones in our study to these findings since these studies also reported that high-complexity aviaries seem to not have the same benefits on pullet keel bones as it has been reported to have on pullet long bones.

It may be expected that pullets reared in high complexity aviary systems present with greater keel bone cortical bone characteristics due to enhanced opportunity for natural mechanical loading, but it is important to mention that pullets reared in aviary systems do not necessarily take advantage of the opportunities to perform natural loading behaviors. Amanda Pufall (2020) reported that pullets (Lohmann Brown and LSL white) spent relatively little of their time locomoting, and that locomotion decreased as the birds reached sexual maturity (16-18 weeks of age) [160]. This study compared pullet locomotion between low, medium, and high complexity aviaries at 4, 10 and 16 weeks of age. The most significant difference in locomotion was seen at 4 weeks of age, with pullets in the high complexity aviary performing more high intensity locomotion than pullets in low complexity aviaries. Although Pufall reported that pullets in the high complexity aviary had proportionally stronger tibiae and femurs, the housing styles had no effect on keel bone area. Jackson et al., 2011 [161] has shown that locomotion including wing-flapping provides mechanical loads to the keel bone, and Casey-Trott et al., 2017a [63] hypothesized that this mechanical load induces keel growth. Since the 4-week-old pullets had the highest activity level and activity decreased thereafter, the effect of high complexity aviary housing after 4 weeks-of-age might not be significant to induce keel bone growth.

3.4.2 No significant difference in microstructural characteristics of fractured and non-fractured keel bones in 30-week-old hens

To my knowledge, this is the first study to report bone microstructural differences in fractured and non-fractured keel bones. Casey-Trott et al.(2017) reported that rearing system and age had an effect on the presence of keel bone fractures in Lohmann LSL-Lite hens [143]. This study showed that hens at 50- and 70-weeks-of-age had increased fracture incidences compared to 30-week-old hens, and that hens reared in aviary systems (Farmer Automatic Portal Pullet rearing system) showed lower fracture incidences (41.6%) than hens reared in conventional cages (60.3%) [143]. Although this study investigated the same genetic strain, at the same age (30-weeks-of-age), and the same aviary system than in our study, it did not report keel bone microstructural data. We showed that no significant interaction was seen between the microstructural characteristics of fractured and non-fractured groups, except for greater trabecular separation in fractured keel bones. Casey-Trott et al.(2017) also reported that 76.9% of keel fractures were located at the caudal tip of the keel bone (within 5 cm of the caudal tip) at 30-weeks-of-age. Although we did not report fracture incidence, location of fractures or type of fractures, we also observed that most fractures were located at the caudal tip in 30-week-old hens. While our study only focused on the microstructural characteristics of fractured and non-fractured keel bones in 30-week-old hens, other students in our lab are conducting the same study on 50-week-old and 70-week-old hens. I believe that these studies, in combination with my study, will allow us to compare keel bone microstructural data to the data Casey-Trott et al.(2017) reported on fracture incidences.

So, since no significant interaction was seen between fractured and non-fractures keel bone microstructure, it may indicate that pullets experiencing keel bone fractures at this age, may not suffer from deteriorated keel bone microstructural parameters, but that keel bone fractures are rather caused by other factors such as altered material properties or whole bone geometry.

3.4.3 Potential relationship between genetic strain and keel bone microstructural properties

The results of our study showed that brown birds had greater total bone area compared to white birds, which may correlate with their greater body weight. Yet this larger bone area in brown birds is associated with greater trabecular separation. Is this due to the shape of the keel bone? The keel bone cross-sectional shape replicates the shape of a 'T', with the top of the 'T' being the metasternum and the bottom being the spine of the keel. With the spine of the keel being much thinner than the metasternum, trabecular bone was more commonly found in the metasternum than in the spine. At the tip of the spine (the bottom of the 'T'), some keel bones had trabecular bone, which meant that trabecular bone was distributed at both ends of the keel bone. How this affected the trabecular separation outcome in this study is not clear. To adequately test if the greater trabecular separation is due to the shape of the keel bone, future studies analyzing and comparing the different regions of the keel bone is required. The greater trabecular separation and reduced trabecular number seen in brown birds, may also be a consequence of the great total area observed in these keel bones. Because of brown birds' greater total bone area, the cortical area fraction is greater in white birds.

3.5 Limitations

The study is not without limitations. Factors that may have influenced the chicken study was fracture status. Although some birds presented with non-fractured keel bones at 30-weeks-of-age, evaluated by radiographic imaging, they may have experienced keel bone fractures earlier in life that have healed by the time they were imaged and grouped. Analysis of μCT images revealed that some keel bones classified as non-fractured keel bones had callus at previous fracture sites. Also, extreme deformities were seen in these keel bones, which may have influenced the study.

Another factor that may have influenced the microstructural bone outcomes in this study is how we characterized trabecular bone. In the keel bone, the difference between trabecular and medullary bone has not yet been well characterized, so it might be possible that the spongy structure within the keel consist of a mix of spongy medullary bone and/or trabecular bone. Further investigation on the localization and structural differences between medullary and trabecular bone is necessary to report accurate microstructural bone outcomes.

3.6 Conclusion

In summary, my research showed that rearing styles do have an effect on the microstructural bone parameters of the keel bone. Surprisingly, the effect of rearing styles on the keel bone microstructure was in contrary to what has been reported on the effect of rearing styles on the microstructural bone parameters of the tibiotarsus. It is evident that birds reared in conventional cages had greater cortical and trabecular keel bone parameters than birds reared in high complexity aviaries. We also showed that brown birds had greater body weight and that their keel bones had greater total bone area compared to white birds. Despite our limitations, we observed greater trabecular separation in fractured keel bones compared to non-fractured keel bones. These data will be helpful for poultry farmers to know which level of complexity may be beneficial for a particular genetic strain to reduce keel bone fracture incidences.

3.7 Figures and tables

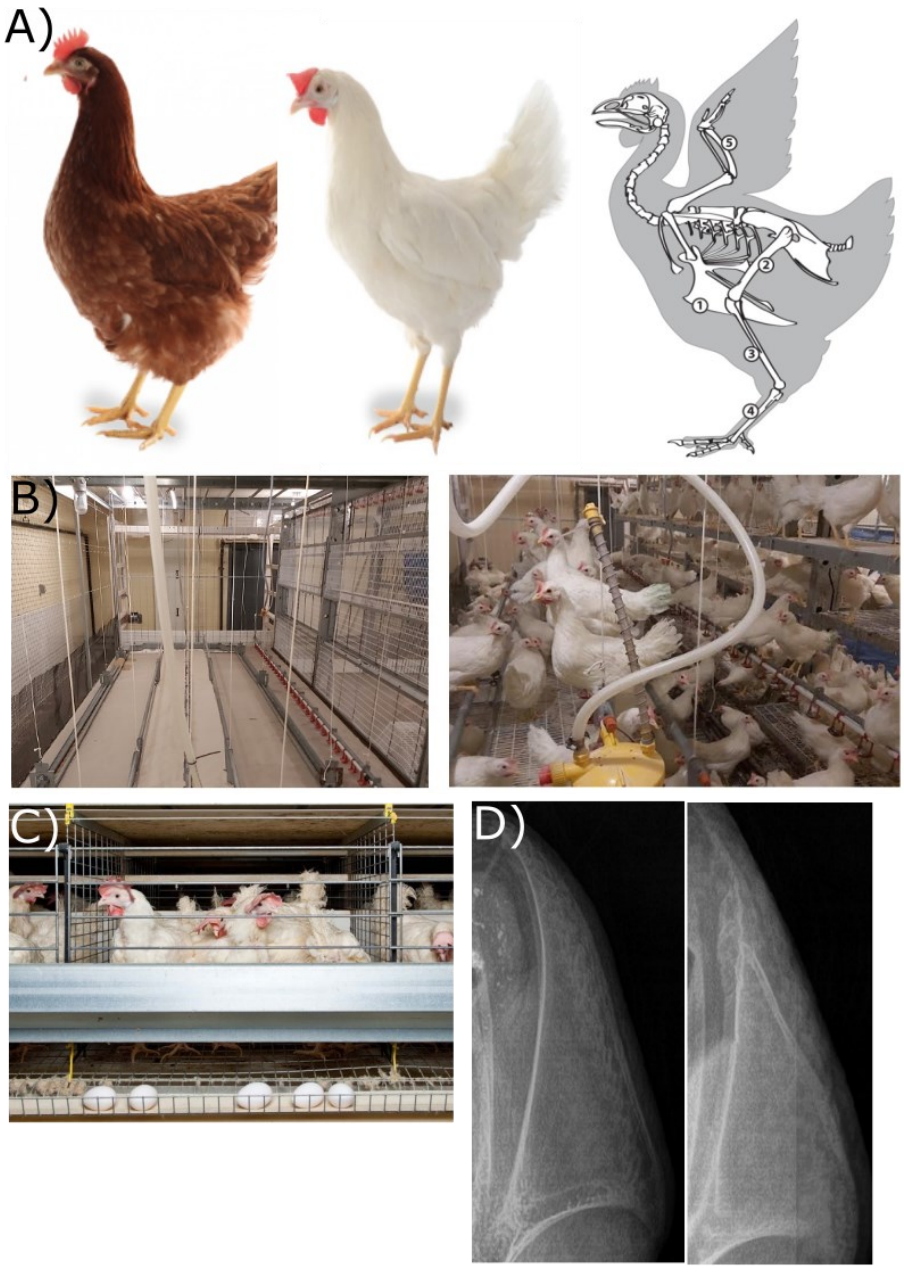

Figure 4: Experimental design. A) Genetic strains used in this study (left and middle): Lohmann Brown-Lite (brown) and LSL-lite (white), illustration of bird anatomy (right): (1)representing the keel bone. B) High complexity aviary housing style (left – image of entire system without birds, right – image of a section of the system after stocking birds) and C) conventional cages. D) Examples of radiograph of a non-fractured (left) and fractured (right) keel bone, used to group birds into sample groups.

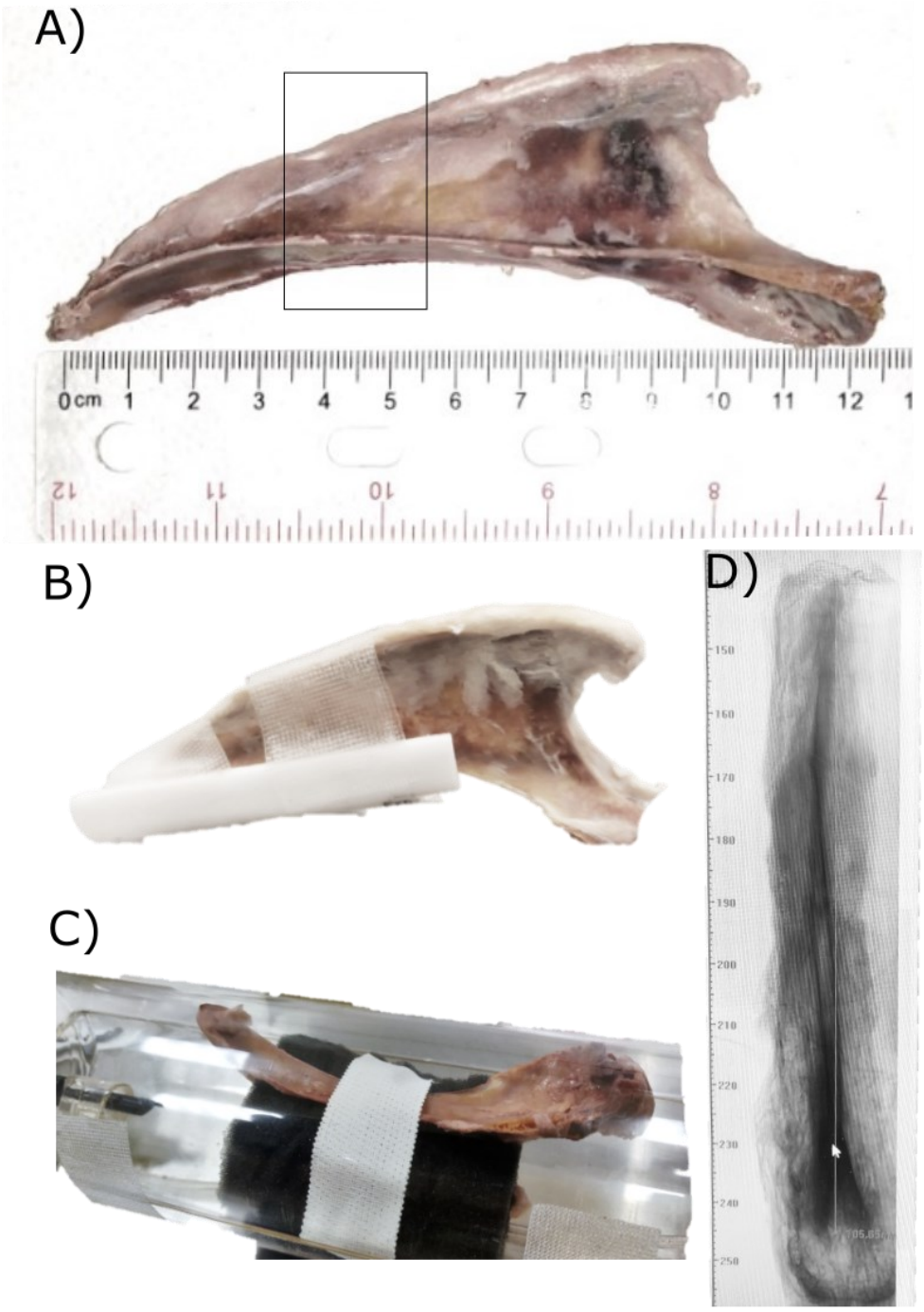

Figure 5: Keel bone preparation and µCT scanning. A) Illustration of VOI of keel bone analyzed B) Splint used to protect the keel tip during scanning C) illustration of how the keel bone was positioned in the scanner cassette (with the metasternum facing upwards, the caudal tip and cranial area parallel to the cassette, the spine of the keel held in place with foam and tape). This is only for illustration purposes. The keel bone was kept in a towel, soaked in 70% ethanol, and bagged during scanning. D) example of the scout view of the entire keel bone scan. The arrow points to the spine of the keel.

Table 1: Cortical (Ct) bone parameters of the keel bone at the midpoint of the keel, determined by in vivo µCT, in brown and white chickens reared in conventional cages (CC) and high-complexity aviaries (HCA). At 30-weeks-of-age, birds were grouped into fractured and non-fractured group. (Mean±SD); between-subject effect of a) genetic strain (brown, white), b) housing system (CC, HCA), c) fracture status (non-fractured, fractured), interactions between d) breed * housing, e) housing * status, f) breed * status; $p < 0.05$ assessed using a repeated measures ANOVA.

	Brown				White			
	CC		HCA		CC		HCA	
Outcome	Non-fractured	Fractured	Non-fractured	Fractured	Non-fractured	Fractured	Non-fractured	Fractured
30-week-old	(n=7)	(n=7)	(n=7)	(n=6)	(n=7)	(n=7)	(n=7)	(n=7)
Imax (mm4)	135 ± 57	142 ± 42	136 ± 40	172 ± 67	151 ± 39	129 ± 43	150 ± 47	107 ± 63
Imin (mm4) a	35 ± 15	40 ± 9	37 ± 12	42 ± 10	21 ± 12	19 ± 6	24 ± 6	17 ± 4
Ct.Ar (mm2) b	5.26 ± 1.20	5.62 ± 0.29	5.02 ± 0.90	4.59 ± 1.06	5.35 ± 1.31	4.75 ± 0.97	5.03 ± 1.59	3.76 ± 1.30
Tt.Ar (mm2) a	21.81 ± 3.25	21.67 ±3.08	22.29 ±5.79	22.59 ± 2.10	15.77 ±5.37	14.29 ±1.36	17.25 ±3.30	16.63 ±1.67
Ct.Ar/Tt.Ar (mm2/mm2)a,b	0.24 ± 0.06	0.26 ± 0.03	0.24 ± 0.07	0.21 ± 0.06	0.37 ± 0.14	0.33 ± 0.07	0.31 ± 0.14	0.22 ± 0.06
Ma.Ar (mm2) a	16.55 ± 3.15	16.04 ±3.05	17.27 ±5.73	17.99 ± 3.03	10.41 ±5.59	9.54 ±1.72	12.22 ±4.29	12.88 ±1.11
Ct.Th (mm)b	0.17 ± 0.03	0.17 ± 0.03	0.15 ± 0.03	0.16 ± 0.03	0.18 ± 0.04	0.16 ± 0.02	0.16 ± 0.04	0.13 ± 0.02
Ct.vTMD (mg HA/cm3) b,e	0.55 ± 0.12	0.63 ± 0.04	0.57 ± 0.07	0.55 ± 0.1	0.63 ± 0.06	0.65 ± 0.08	0.62 ± 0.05	0.53 ± 0.12

Table 2: Trabecular (Tb) bone parameters of the keel bone at the midpoint of the keel, determined by in vivo µCT, in brown and white chickens reared in conventional cages (CC) and high-complexity aviaries (HCA). At 30-weeks-of-age, birds were grouped into fractured and non-fractured group. (Mean±SD); between-subject effect of a) genetic strain (brown, white), b) housing system (CC, HCA), c) fracture status (non-fractured, fractured), interactions between d) breed * housing, e) housing * status, f) breed * status; $p < 0.05$ assessed using a repeated measures ANOVA.

	Brown				White			
	CC		HCA		CC		HCA	
Outcome	Non-fractured	Fractured	Non-fractured	Fractured	Non-fractured	Fractured	Non-fractured	Fractured
30-week-old	(n=7)	(n=7)	(n=7)	(n=6)	(n=7)	(n=7)	(n=7)	(n=7)
Tb.BV/TV (mm3/mm3)b	0.12 ± 0.11	0.10 ± 0.05	0.10 ± 0.08	0.05 ± 0.03	0.21 ± 0.15	0.15 ± 0.12	0.14 ± 0.13	0.07 ± 0.06
Tb.Th (µm)b	0.08 ± 0.02	0.09 ± 0.01	0.07 ± 0.01	0.08 ± 0.01	0.09 ± 0.02	0.08 ± 0.01	0.07 ± 0.01	0.07 ± 0.01
Tb.N (1/mm)	1.40 ± 1.22	1.20 ± 0.59	1.24 ± 1.05	0.65 ± 0.32	2.28 ± 1.42	1.78 ± 1.34	1.67 ± 1.35	0.94 ± 0.77
Tb.Sp (µm)a,c	0.46 ± 0.29	0.52 ± 0.14	0.34 ± 0.2	0.74 ± 0.22	0.31 ± 0.16	0.38 ± 0.18	0.35 ± 0.14	0.49 ± 0.15
Tb.vTMD (mg HA/cm3)b	0.55 ± 0.04	0.59 ± 0.02	0.53 ± 0.02	0.56 ± 0.03	0.57 ± 0.04	0.58 ± 0.05	0.55 ± 0.03	0.56 ± 0.04

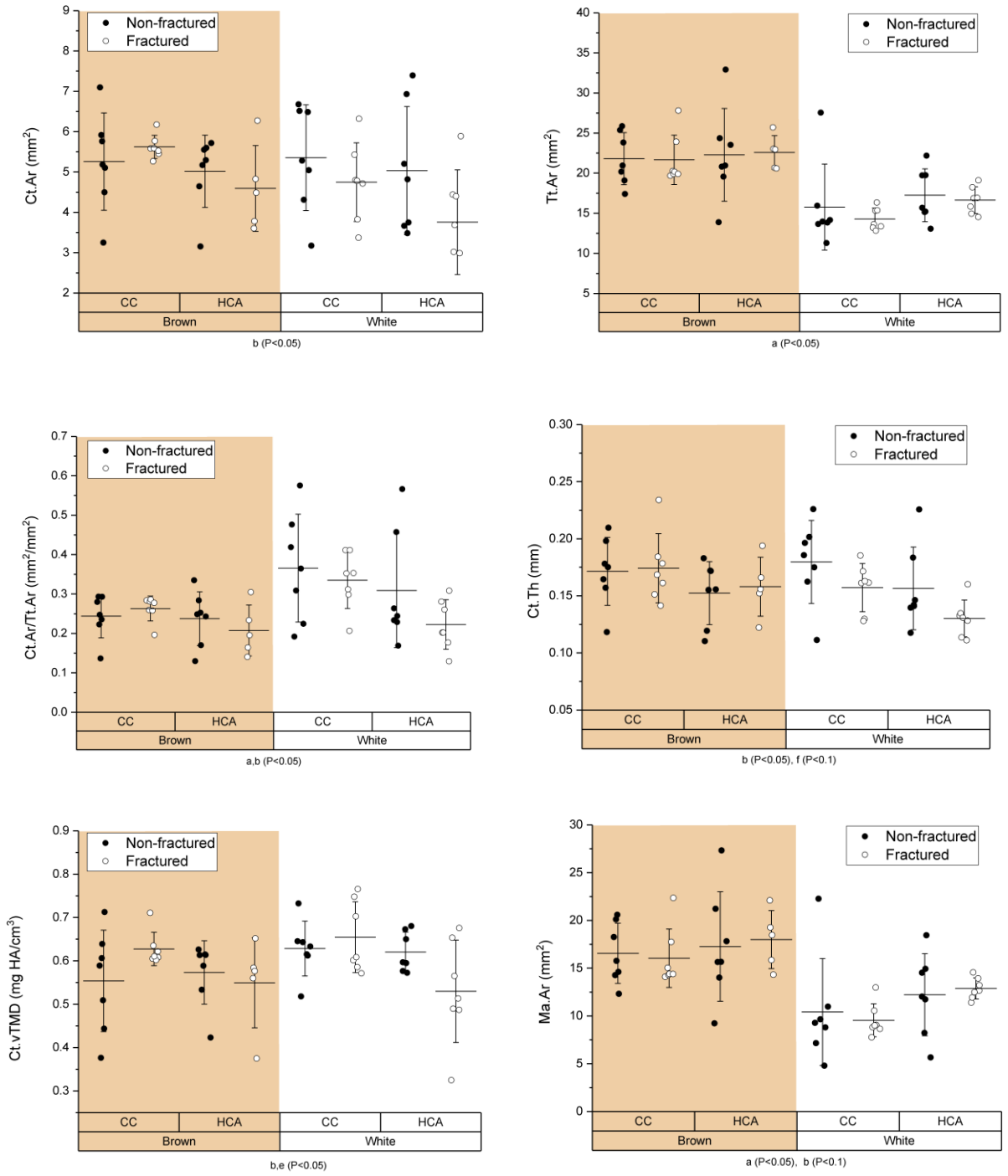

Figure 6: µCT image analysis of the keel bone cortical parameters (Ct.Ar, Tt.Ar, Ct.Ar/Tt.Ar, Ct.Th, Ct.vTMD, Ma.Ar) in brown and white birds, reared in conventional cages (CC) and high complexity aviaries (HCA), and in both fractured and non-fractured groups. ANOVA main effects: (a) Genetic strain; (b) Housing; (c) Status, (d) Breed*Housing, (e) Housing*Status, (f) Breed * Status, followed by paired t-test: (*) $p < 0.05$

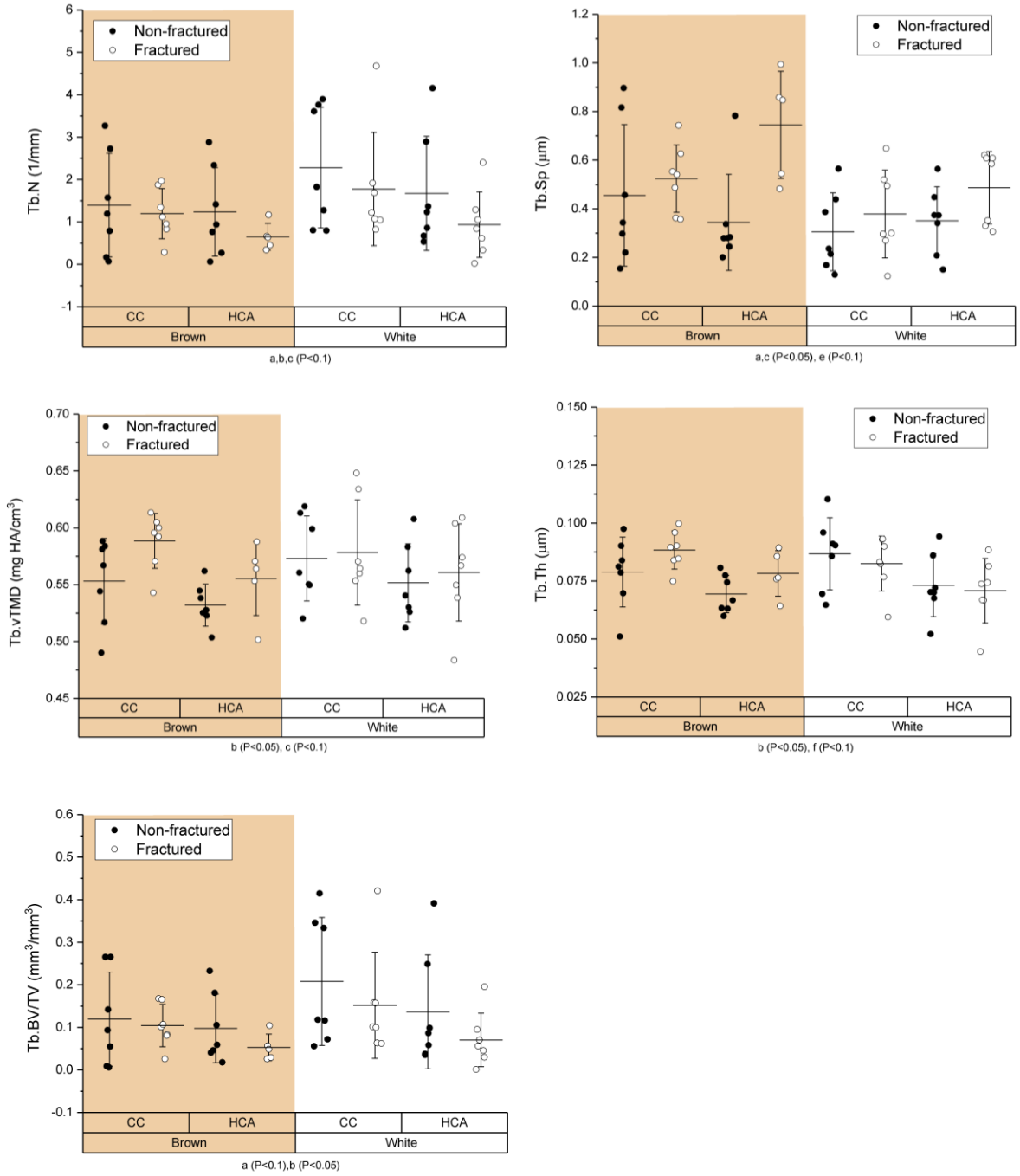

Figure 7: µCT image analysis of the keel bone trabecular parameters (Tb.N, Tb.Sp, Tb.Th, Tb.vTMD, Tb.BV/TV) in brown and white birds, reared in conventional cages (CC) and high complexity aviaries (HCA), and in both fractured and non-fractured groups. ANOVA main effects: (a) Genetic strain; (b) Housing; (c) Status, (d) Breed*Housing, (e) Housing*Status, (f) Breed * Status, followed by paired t-test: (*) $p < 0.05$.

Table 4**:** Body weight and length of the keel bone in brown and white chickens reared in conventional cages (CC) and high-complexity aviaries (HCA). At 30-weeks-of-age, birds were weighed immediately after euthanasia and the keel bone length was measured after dissection. Results include the Mean±SD; between-subject effect of a) genetic strain (brown, white), b) housing system (CC, HCA), c) fracture status (non-fractured, fractured), interactions between d) breed * housing, e) housing * status, f) breed * status; $p < 0.05$ assessed using a repeated measures ANOVA.

	Brown				White			
	CC		HCA		CC		HCA	
Outcome	Non-fractured	Fractured	Non-fractured	Fractured	Non-fractured	Fractured	Non-fractured	Fractured
30-week-old	(n=7)	(n=7)	(n=7)	(n=6)	(n=7)	(n=7)	(n=7)	(n=7)
Body weight (g)a	2058 ± 288	2146 ±207	2084 ± 154	2101 ± 248	1765 ± 203	1736 ± 151	1779 ± 158	1669 ± 125
Keel length (mm)	94.35±15.03	98.09 ±4.48	98.92 ±6.45	96.10 ± 4.76	93.81 ±5.35	93.99 ±3.63	97.00 ±3.01	95.36 ±2.31

Global discussion

How the COVID-19 pandemic influenced this study

I began my MEng research in January 2020, at which time the Gorab mice study commenced. We were able to conduct the loading experiment and µCT scanning before the lockdown restrictions were imposed in March 2020 due to the COVID-19 pandemic. During this lockdown period, µCT scans were analyzed remotely. It was only in July 2020 that we could return to our lab to continue with bench work, which included embedding the mice tibiae, cutting embedded samples, and imaging samples with a confocal microscope. These procedures all required training that was also delayed or unavailable during the pandemic. By September 2020, the gene expression analysis could be conducted to determine the *Gorab* knockout level in these mice. It was only by October 2020 that we established that the level of *Gorab* knockout in these inducible knockout mice were unsuccessful. By this time, the µCT analyses and preparation of the samples for histomorphometry had been performed. However, at this point I stopped all work on this cohort of mice and we decided to repeat the study in the future, after further testing of tamoxifen protocols to improve our knockdown efficiency. The timeline of when we would be able to receive new mice from Charité - Universitätsmedizin Berlin, Germany, for breeding was still unclear under the pandemic restrictions of that time, therefore we decided that I start working on another project involving chickens since these specimens were readily available from our collaborators at the University of Guelph (see Chapter 3). In January 2021, mice arrived from Charité, and we commenced breeding. I am currently determining an effective tamoxifen dosage; however, this data will not be included in my thesis.

Future work

For the Gorab mice study, we aim to determine an effective tamoxifen dose that can be used to successfully repeat the study. If we achieve significant knockdown levels, we can not only investigate the static bone morphometry, but also the bone histomorphometry. The two-week in vivo loading and in vivo µCT imaging on day 0, 5, 10 and 15 can be repeated to determine if the tamoxifen-treated mice had a similar response to loading as the vehicle-treated mice. Further we can investigate the bone apposition rate differences between these group and look at images of the OLCN of these mice. These results can be compared to the findings of the previous study, which reported an altered OLCN in Gorab^{Prx1} mice. This will contribute to a larger Gorab study that is ongoing and will help to better understand what effect the loss-of-function mutation of the *GORAB* gene has on the mechanoresponse of bone in GO patients.

For the chicken study, further analysis of the keel bone using histomorphometry can be performed to determine the rate of bone formation. These chickens received calcein injections prior to euthanasia and their keel bones have been prepped for embedding. We can also use TRAP staining to examine bone resorption. Additionally, the material properties of the bone and whole bone geometry will be investigated. The chicken study included in this thesis only focusses on the 30-week-old age group, while the larger project performed by other graduate students will also analyze the keel bone microstructure of these hens at 50-weeks-of-age and at 70-weeks-of-age. Studies are also being performed by other graduate students in our lab examining microstructural properties in the tibiotarsus from all three age groups. This will shed light on the bone properties of both the keel bone and tibiotarsus at

three stages of the laying hen's life. We are also interested to see if the keel bone adapts to mechanical loading or aviary rearing similarly than the tibiotarsus. Besides the microstructural analysis of the keel bone, other studies on the effect of pectoralis muscle strain or slower ossification of the keel bone could shed light on the mechanoadaptation of the keel bone to better understand the causes of keel bone fractures. I believe that the larger project will contribute to a better understanding of the long-term bone health of aviary rearing in laying hens, and that it can aid to implement better housing systems for the welfare of egg-laying hens.

References

[1] D. B. Burr and O. Akkus, *Bone Morphology and Organization*. Elsevier Inc., 2013.

[2] T. Bellido, L. I. Plotkin, and A. Bruzzaniti, "Bone Cells," *Basic Appl. Bone Biol.*, vol. 14, pp. 27–45, 2013, doi: 10.1016/B978-0-12-416015-6.00002-2.

[3] M. Rupp, F. Merboth, D. E. Daghma, C. Biehl, T. El Khassawna, and C. Hei β, "Osteocytes," *Z. Orthop. Unfall.*, vol. 157, no. 2, pp. 154–162, 2019, doi: 10.1055/a-0658-5922.

[4] S. L. Dallas, Y. Xie, L. A. Shiflett, and Y. Ueki, "Mouse Cre Models for the Study of Bone Diseases," doi: 10.1007/s11914-018-0455-7.

[5] S. Tatsumi *et al.*, "Targeted Ablation of Osteocytes Induces Osteoporosis with Defective Mechanotransduction," *Cell Metab.*, vol. 5, no. 6, pp. 464–475, Jun. 2007, doi: 10.1016/j.cmet.2007.05.001.

[6] N. BS *et al.*, "Mechanical loading: biphasic osteocyte survival and targeting of osteoclasts for bone destruction in rat cortical bone," *Am. J. Physiol. Cell Physiol.*, vol. 284, no. 4, Apr. 2003, doi: 10.1152/AJPCELL.00234.2002.

[7] J. RL, "The relevance of mouse models for investigating age-related bone loss in humans," *J. Gerontol. A. Biol. Sci. Med. Sci.*, vol. 68, no. 10, pp. 1209–1217, Oct. 2013, doi: 10.1093/GERONA/GLT046.

[8] Y. R *et al.*, "Aging in inbred strains of mice: study design and interim report on median lifespans and circulating IGF1 levels," *Aging Cell*, vol. 8, no. 3, pp. 277–287, 2009, doi: 10.1111/J.1474-9726.2009.00478.X.

[9] C. Ackert-Bicknell, W. . Beamer, C. . Rosen, and J. . Sundburg, "Aging Study: Bone Mineral Density and Body Composition of 32 Inbred strains of Mice.," *Mouse*

Phenome Database Website, The Jackson Laboratory. http://phenome.jax.org (accessed Sep. 09, 2021).

[10] P. AM, "Misconceptions (1): epiphyseal fusion causes cessation of growth," *Bone*, vol. 30, no. 2, pp. 337–339, 2002, doi: 10.1016/S8756-3282(01)00668-8.

[11] G. V, C. E, S. L, and B. ML, "Age-related changes in trabecular architecture differ in female and male C57BL/6J mice," *J. Bone Miner. Res.*, vol. 22, no. 8, pp. 1197–1207, Aug. 2007, doi: 10.1359/JBMR.070507.

[12] P. AM, "Osteonal and hemi-osteonal remodeling: the spatial and temporal framework for signal traffic in adult human bone," *J. Cell. Biochem.*, vol. 55, no. 3, pp. 273–286, 1994, doi: 10.1002/JCB.240550303.

[13] M. Piemontese *et al.*, "Old age causes de novo intracortical bone remodeling and porosity in mice," *JCI Insight*, vol. 2, no. 17, Sep. 2017, doi: 10.1172/JCI.INSIGHT.93771.

[14] P. AM, "Misconceptions (2): turnover is always higher in cancellous than in cortical bone," *Bone*, vol. 30, no. 6, pp. 807–809, 2002, doi: 10.1016/S8756-3282(02)00735-4.

[15] W. RS, J. RL, P. AM, and M. SC, "Inhibition of osteoblastogenesis and promotion of apoptosis of osteoblasts and osteocytes by glucocorticoids. Potential mechanisms of their deleterious effects on bone," *J. Clin. Invest.*, vol. 102, no. 2, pp. 274–282, Jul. 1998, doi: 10.1172/JCI2799.

[16] P. AM, H. ZH, P. S, R. DS, S. MS, and N. D, "Effects of ethnicity and age or menopause on osteoblast function, bone mineralization, and osteoid accumulation in iliac bone," *J. Bone Miner. Res.*, vol. 12, no. 11, pp. 1864–1873, 1997, doi: 10.1359/JBMR.1997.12.11.1864.

[17] K. S, "Pathogenesis of age-related bone loss in humans," *J. Gerontol. A. Biol. Sci. Med. Sci.*, vol. 68, no. 10, pp. 1226–1235, Oct. 2013, doi: 10.1093/GERONA/GLS163.

[18] H. BP, F. VL, S. SJ, B. A, V. LL, and M. S, "Changes in bone structure and mass with advancing age in the male C57BL/6J mouse," *J. Bone Miner. Res.*, vol. 17, no. 6, pp. 1044–1050, Jan. 2002, doi: 10.1359/JBMR.2002.17.6.1044.

[19] S. E, "Pathogenesis of bone fragility in women and men," *Lancet (London, England)*, vol. 359, no. 9320, pp. 1841–1850, May 2002, doi: 10.1016/S0140-6736(02)08706-8.

[20] K. E. Kittelsen, P. Jensen, J. P. Christensen, I. Toftaker, R. O. Moe, and G. Vasdal, "Prevalence of keel bone damage in red jungle fowls (Gallus gallus)—a pilot study," *Animals*, vol. 10, no. 9, pp. 1–8, Sep. 2020, doi: 10.3390/ani10091655.

[21] M. Toscano, "Skeletal problems in contemporary commercial laying hens," in *Advances in Poultry Welfare*, Elsevier, 2017, pp. 151–173.

[22] S. Käppeli, S. G. Gebhardt-Henrich, E. Fröhlich, A. Pfulg, and M. H. Stoffel, "Prevalence of keel bone deformities in Swiss laying hens," *Br. Poult. Sci.*, vol. 52, no. 5, pp. 531–536, 2011, doi: 10.1080/00071668.2011.615059.

[23] R. Freire, L. J. Wilkins, F. Short, and C. J. Nicol, "Behaviour and welfare of individual laying hens in a non-cage system," *http://dx.doi.org.proxy3.library.mcgill.ca/10.1080/0007166031000085391*, vol. 44, no. 1, pp. 22–29, Mar. 2010, doi: 10.1080/00071660310000853 91.

[24] R. TB, T. FA, S. B, D. R. K, H. L, and Z. J, "Welfare, health, and hygiene of laying hens housed in furnished cages and in alternative housing systems," *J. Appl. Anim. Welf. Sci.*, vol. 8, no. 3, pp. 211–226, 2005, doi: 10.1207/S15327604JAWS0803_5.

[25] L. J. Wilkins *et al.*, "Papers: Influence of housing system and design on bone strength and keel bone fractures in laying hens," *Vet. Rec.*, vol. 169, no. 16, p. 414, Oct. 2011, doi: 10.1136/vr.d4831.

[26] C. C. Whitehead, "Overview of bone biology in the egg-laying hen," in *Poultry Science*, Feb. 2004, vol. 83, no. 2, pp. 193–199, doi: 10.1093/ps/83.2.193.

[27] B. A. Kamp and M. A. Grashorn, "Determination of the ossification process of fast and slow growing broilers," pp. 23–26, 2005.

[28] M. Kerschnitzki, T. Zander, P. Zaslansky, P. Fratzl, R. Shahar, and W. Wagermaier, "Rapid alterations of avian medullary bone material during the daily egg-laying cycle," *Bone*, vol. 69, pp. 109–117, Dec. 2014, doi: 10.1016/J.BONE.2014.08.019.

[29] B. M. Willie, E. A. Zimmermann, I. Vitienes, R. P. Main, and S. V. Komarova, "Bone adaptation: Safety factors and load predictability in shaping skeletal form," *Bone*, vol. 131. Elsevier Inc., p. 115114, Feb. 01, 2020, doi: 10.1016/j.bone.2019.115114.

[30] J. Wolff, *The Law of Bone Transformation*, Springer,. Berlin, 1892.

[31] L. F. Bonewald, "The amazing osteocyte," *J. Bone Miner. Res.*, vol. 26, no. 2, pp. 229–

238, Feb. 2011, doi: 10.1002/jbmr.320.

[32] P. D *et al.*, "Sost deficiency led to a greater cortical bone formation response to mechanical loading and altered gene expression," *Sci. Rep.*, vol. 7, no. 1, Dec. 2017, doi: 10.1038/S41598-017-09653-9.

[33] N. T *et al.*, "Evidence for osteocyte regulation of bone homeostasis through RANKL expression," *Nat. Med.*, vol. 17, no. 10, pp. 1231–1234, Oct. 2011, doi: 10.1038/NM.2452.

[34] T. A and Z. A, "Do osteocytes contribute to bone mineral homeostasis? Osteocytic osteolysis revisited," *Bone*, vol. 44, no. 1, pp. 11–16, Jan. 2009, doi: 10.1016/J.BONE.2008.09.017.

[35] H. Hemmatian, A. D. Bakker, J. Klein-Nulend, and G. H. van Lenthe, "Aging, Osteocytes, and Mechanotransduction," *Current Osteoporosis Reports*, vol. 15, no. 5. Current Medicine Group LLC 1, pp. 401–411, Oct. 01, 2017, doi: 10.1007/s11914-017-0402-z.

[36] M. R. Forwood, "Growing a Healthy Skeleton: The Importance of Mechanical Loading," *Prim. Metab. Bone Dis. Disord. Miner. Metab. Eighth Ed.*, pp. 149–155, 2013, doi: 10.1002/9781118453926.ch19.

[37] S. Srinivasan, T. S. Gross, and S. D. Bain, "Bone Mechanotransduction May Require Augmentation in Order to Strengthen the Senescent Skeleton," 2011, doi: 10.1016/j.arr.2011.12.007.

[38] A. I. Birkhold, H. Razi, G. N. Duda, R. Weinkamer, S. Checa, and B. M. Willie, "The influence of age on adaptive bone formation and bone resorption," *Biomaterials*, vol. 35, no. 34, pp. 9290–9301, Nov. 2014, doi: 10.1016/j.biomaterials.2014.07.051.

[39] H. M. Frost, "On Our Age-Related Bone Loss: Insights from a New Paradigm," *J. Bone Miner. Res.*, vol. 12, no. 10, pp. 1539–1546, Oct. 1997, doi: 10.1359/JBMR.1997.12.10.1539.

[40] F. Pauwels, "Gesammelte Abjandlungen zur Funktionellen Anatomie des Bewegungsapparates," *Br. J. Surg.*, vol. 53, no. 9, pp. 831–831, 1965.

[41] T. Lu, S. J. . Taylor, J. O'Connor, and P. . Walker, "Influence of muscle activity on the forces in the femur: an in vivo study," *Biomechanics*, vol. 30, no. 11, pp. 1101–1106,

1997.

[42] K. H. Myburgh, S. Charette, L. Zhou, C. Steele, S. Arnaud, and R. Marcus, “Influence of recreational activity and muscle strength on ulnar ending stiffness in men,” *Med. Sci. Sport. Exerc.*, vol. 25, no. 5, pp. 592–596, 1993.

[43] M. L. Villa, R. Marcus, R. R. Delay, and J. L. Kelsey, “Factors contributing to skeletal health of postmenopausal Mexican-American women,” *J. Bone Miner. Res.*, vol. 10, no. 8, pp. 1233–1242, Aug. 1995, doi: 10.1002/JBMR.5650100814.

[44] H. Sievänen, A. Heinonen, and P. Kannus, “Adaptation of bone to altered loading environment: a biomechanical approach using x-ray absorptiometric data from the patella of a young woman,” *Bone*, vol. 19, no. 1, pp. 55–59, Jul. 1996, doi: 10.1016/8756-3282(96)00111-1.

[45] E. Schönau *et al.*, “Influence of Muscle Strength on Bone Strength during Childhood and Adolescence,” *Horm. Res. Paediatr.*, vol. 45, no. Suppl. 1, pp. 63–66, 1996, doi: 10.1159/000184834.

[46] H. M. Frost, *Intermediary Organization of the Skeleton*. Boca Raton,FL, USA: CRC Press, 1986.

[47] D. B. Burr, “Muscle Strength, Bone Mass, and Age-Related Bone Loss,” *J. Bone Miner. Res.*, vol. 12, no. 10, pp. 1547–1551, Oct. 1997, doi: 10.1359/JBMR.1997.12.10.1547.

[48] R. P. Main, S. J. Shefelbine, L. B. Meakin, M. J. Silva, M. C. H. van der Meulen, and B. M. Willie, “Murine Axial Compression Tibial Loading Model to Study Bone Mechanobiology: Implementing the Model and Reporting Results,” *J. Orthop. Res.*, vol. 38, no. 2, pp. 233–252, Feb. 2020, doi: 10.1002/JOR.24466.

[49] R. P. Main, S. J. Shefelbine, L. B. Meakin, M. J. Silva, M. C. H. van der Meulen, and B. M. Willie, “Murine Axial Compression Tibial Loading Model to Study Bone Mechanobiology: Implementing the Model and Reporting Results,” *J. Orthop. Res.*, vol. 38, no. 2, pp. 233–252, Feb. 2020, doi: 10.1002/JOR.24466.

[50] S. D, B. MD, Z. HM, H. N, and S. MJ, “Evaluation of loading parameters for murine axial tibial loading: Stimulating cortical bone formation while reducing loading duration,” *J. Orthop. Res.*, vol. 36, no. 2, pp. 682–691, Feb. 2018, doi: 10.1002/JOR.23727.

[51] B. M. Willie *et al.*, "Diminished response to in vivo mechanical loading in trabecular and not cortical bone in adulthood of female C57Bl/6 mice coincides with a reduction in deformation to load ☆," *Orig. Full Length Artic.*, 2013, doi: 10.1016/j.bone.2013.04.023.

[52] H. N, B. MD, S. ME, K. AA, and S. MJ, "Adaptation of tibial structure and strength to axial compression depends on loading history in both C57BL/6 and BALB/c mice," *Calcif. Tissue Int.*, vol. 93, no. 3, pp. 211–221, Sep. 2013, doi: 10.1007/S00223-013-9744-4.

[53] B. M. Willie *et al.*, "Diminished response to in vivo mechanical loading in trabecular and not cortical bone in adulthood of female C57Bl/6 mice coincides with a reduction in deformation to load," *Bone*, vol. 55, no. 2, pp. 335–346, Aug. 2013, doi: 10.1016/j.bone.2013.04.023.

[54] H. N, B. MD, S. ME, and S. MJ, "Aging diminishes lamellar and woven bone formation induced by tibial compression in adult C57BL/6," *Bone*, vol. 65, pp. 83–91, 2014, doi: 10.1016/J.BONE.2014.05.006.

[55] L. ME *et al.*, "Tibial compression is anabolic in the adult mouse skeleton despite reduced responsiveness with aging," *Bone*, vol. 49, no. 3, pp. 439–446, Sep. 2011, doi: 10.1016/J.BONE.2011.05.017.

[56] M. J. Silva, M. D. Brodt, M. A. Lynch, A. L. Stephens, and D. J. Wood, "Tibial Loading Increases Osteogenic Gene Expression and Cortical Bone Volume in Mature and Middle-Aged Mice," *PLoS One*, vol. 7, no. 4, p. 34980, 2012, doi: 10.1371/journal.pone.0034980.

[57] M. D. Brodt and M. J. Silva, "Aged Mice Have Enhanced Endocortical Response and Normal Periosteal Response Compared With Young-Adult Mice Following 1 Week of Axial Tibial Compression," *J. Bone Miner. Res.*, vol. 25, no. 9, p. 2006, Sep. 2010, doi: 10.1002/JBMR.96.

[58] C. . Comar and J. . Driggers, "Secretion of radioactive calcium in the hen's eggs," *Science (80-.).*, vol. 109, p. 282, 1949.

[59] W. J. Mueller, R. Schraer, and A. Schraer, "Calcium Metabolism and Skeletal Dynamics of Laying Pullets '." Accessed: Jul. 02, 2021. [Online]. Available: https://academic.oup.com/jn/article/84/1/20/4775499.

[60] A. A. Biewener and J. E. Bertram, “Structural response of growing bone to exercise and disuse,” *https://doi.org/10.1152/jappl.1994.76.2.946*, vol. 76, no. 2, pp. 946–955, 1994, doi: 10.1152/JAPPL.1994.76.2.946.

[61] S. C. Bishop, R. H. Fleming, H. A. Mccormack, D. K. Flock, and C. C. Whitehead, “British Poultry Science Inheritance of bone characteristics affecting osteoporosis in laying hens Inheritance of bone characteristics affecting osteoporosis in laying hens,” 2010, doi: 10.1080/00071660086376.

[62] E. Aguado, F. Pascaretti-Grizon, E. Goyenvalle, M. Audran, and D. Chappard, “Bone mass and bone quality are altered by hypoactivity in the chicken,” *PLoS One*, vol. 10, no. 1, pp. 1–12, 2015, doi: 10.1371/journal.pone.0116763.

[63] T. M. Casey-Trott, D. R. Korver, M. T. Guerin, V. Sandilands, S. Torrey, and T. M. Widowski, “Opportunities for exercise during pullet rearing, Part I: Effect on the musculoskeletal characteristics of pullets,” *Poult. Sci.*, vol. 96, no. 8, pp. 2509–2517, Aug. 2017, doi: 10.3382/PS/PEX059.

[64] L. C, T. B, B. S, and H.-M. A, “Development of locomotion over inclined surfaces in laying hens,” *Animal*, vol. 12, no. 3, pp. 585–596, Mar. 2018, doi: 10.1017/S1751731117001896.

[65] P. Regmi, N. Smith, N. Nelson, R. C. Haut, M. W. Orth, and D. M. Karcher, “Housing conditions alter properties of the tibia and humerus during the laying phase in Lohmann white Leghorn hens 1,” *Poult. Sci.*, vol. 95, pp. 198–206, 2016, doi: 10.3382/ps/pev209.

[66] S. O. Poore, A. Ashcroft, A. Sánchez-Haiman, and G. E. Goslow, “The contractile properties of the M. supracoracoideus In the pigeon and starling: a case for long-axis rotation of the humerus,” *J. Exp. Biol.*, vol. 200, no. 23, pp. 2987–3002, Dec. 1997, doi: 10.1242/JEB.200.23.2987.

[67] K. P. Dial, “Activity patterns of the wing muscles of the pigeon (Columba livia) during different modes of flight,” *J. Exp. Zool.*, vol. 262, no. 4, pp. 357–373, Jul. 1992, doi: 10.1002/JEZ.1402620402.

[68] A. Sokoloff, J. Gray-Chickering, H. JD, P. SO, and G. Goslow, “The function of the supracoracoideus muscle during takeoff in the European starling Sturnus vulgaris: Maxheinz Sy revisited,” *New Perspect. Orig. Early Evol. Birds*, pp. 319–332, 2001.

[69] A. A. Biewener and Roberts, “Muscle and tendon contributions to force, work, and elastic energy savings: a comparative persective,” *Exerc. Sport Sci.*, vol. 28, no. 3, pp. 99–107, 2000.

[70] T. BW and D. KP, “Effects of body size on take-off flight performance in the Phasianidae (Aves),” *J. Exp. Biol.*, vol. 203, no. Pt 21, pp. 3319–3332, 2000, Accessed: Sep. 20, 2021. [Online]. Available: https://pubmed-ncbi-nlm-nih-gov.proxy3.library.mcgill.ca/11023852/.

[71] H. TL, T. BW, and B. AA, “How cockatiels (Nymphicus hollandicus) modulate pectoralis power output across flight speeds,” *J. Exp. Biol.*, vol. 206, no. Pt 8, pp. 1363–1378, Apr. 2003, doi: 10.1242/JEB.00272.

[72] K. P. Dial and A. A. Biewener, “PECTORALIS MUSCLE FORCE AND POWER OUTPUT DURING DIFFERENT MODES OF FLIGHT IN PIGEONS (COLUMBA LIVIA),” *J. Exp. Biol.*, vol. 176, no. 1, pp. 31–54, Mar. 1993, doi: 10.1242/JEB.176.1.31.

[73] M. LJ *et al.*, “Does reduced skeletal loading account for age-related bone loss?,” *J. Bone Miner. Res.*, vol. 21, no. 12, pp. 1847–1855, Dec. 2006, doi: 10.1359/JBMR.060908.

[74] L. L and S. T, “Postmenopausal osteoporosis as a failure of bone’s adaptation to functional loading: a hypothesis,” *J. Bone Miner. Res.*, vol. 16, no. 11, pp. 1937–1947, 2001, doi: 10.1359/JBMR.2001.16.11.1937.

[75] A. JF, M. DM, V. AN, R. P, and C. SH, “Relationship of menopause to skeletal and muscle mass,” *Am. J. Clin. Nutr.*, vol. 53, no. 6, pp. 1378–1383, 1991, doi: 10.1093/AJCN/53.6.1378.

[76] K. DA, P. CC, and T. JD, “The role of muscle loss in the age-related decline of grip strength: cross-sectional and longitudinal perspectives,” *J. Gerontol.*, vol. 45, no. 3, 1990, doi: 10.1093/GERONJ/45.3.M82.

[77] K. S, S. H, K. P, P. M, and V. I, “Effect of long-term impact-loading on mass, size, and estimated strength of humerus and radius of female racquet-sports players: a peripheral quantitative computed tomography study between young and old starters and controls,” *J. Bone Miner. Res.*, vol. 17, no. 12, pp. 2281–2289, Dec. 2002, doi: 10.1359/JBMR.2002.17.12.2281.

[78] F. RK, B. JJ, and S. CM, “Jumping improves hip and lumbar spine bone mass in

prepubescent children: a randomized controlled trial," *J. Bone Miner. Res.*, vol. 16, no. 1, pp. 148–156, 2001, doi: 10.1359/JBMR.2001.16.1.148.

[79] H. A *et al.*, "Randomised controlled trial of effect of high-impact exercise on selected risk factors for osteoporotic fractures," *Lancet (London, England)*, vol. 348, no. 9038, pp. 1343–1347, Nov. 1996, doi: 10.1016/S0140-6736(96)04214-6.

[80] K. T, T. T, Y. T, H. Y, H. A, and U. Y, "Effect of low-repetition jump training on bone mineral density in young women," *J. Appl. Physiol.*, vol. 100, no. 3, pp. 839–843, Mar. 2006, doi: 10.1152/JAPPLPHYSIOL.00666.2005.

[81] V. A, K. R, V. E, R.-P. A, L. J, and J. T, "Intensity of exercise is associated with bone density change in premenopausal women," *Osteoporos. Int.*, vol. 17, no. 3, pp. 455–463, Mar. 2006, doi: 10.1007/S00198-005-0005-X.

[82] V. A, K. R, L. J, and J. T, "Effects of high-impact exercise on bone mineral density: a randomized controlled trial in premenopausal women," *Osteoporos. Int.*, vol. 16, no. 2, pp. 191–197, Feb. 2005, doi: 10.1007/S00198-004-1659-5.

[83] K. D, M. A, D. I, and P. R, "Exercise effects on bone mass in postmenopausal women are site-specific and load-dependent," *J. Bone Miner. Res.*, vol. 11, no. 2, pp. 218–225, 1996, doi: 10.1002/JBMR.5650110211.

[84] K. WM, E. AA, and B. SJ, "Effects of exercise involving predominantly either joint-reaction or ground-reaction forces on bone mineral density in older women," *J. Bone Miner. Res.*, vol. 12, no. 8, pp. 1253–1261, Aug. 1997, doi: 10.1359/JBMR.1997.12.8.1253.

[85] K. WM, S. DB, S. E, and B. SJ, "Additive effects of weight-bearing exercise and estrogen on bone mineral density in older women," *J. Bone Miner. Res.*, vol. 10, no. 9, pp. 1303–1311, 1995, doi: 10.1002/JBMR.5650100906.

[86] B. EJ, R. MC, L. JJ, and P. DW, "Pre- and postmenopausal women have different bone mineral density responses to the same high-impact exercise," *J. Bone Miner. Res.*, vol. 13, no. 12, pp. 1805–1813, 1998, doi: 10.1359/JBMR.1998.13.12.1805.

[87] H. A, W. H, C. M, and I. Y, "Effects of exercise at different ages on bone density and mechanical properties of femoral bone of aged mice," *Tohoku J. Exp. Med.*, vol. 185, no. 1, pp. 15–24, 1998, doi: 10.1620/TJEM.185.15.

[88] S. M *et al.*, "Long-term physical exercise retards trabecular bone loss in lumbar vertebrae of aging female mice," *Calcif. Tissue Int.*, vol. 46, no. 2, pp. 80–93, Feb. 1990, doi: 10.1007/BF02556091.

[89] J. TL *et al.*, "Femoral neck response to exercise and subsequent deconditioning in young and adult rats," *J. Bone Miner. Res.*, vol. 18, no. 7, pp. 1292–1299, Jul. 2003, doi: 10.1359/JBMR.2003.18.7.1292.

[90] R. DM, S. EL, C. TD, and T. DP, "Bone mechanical properties after exercise training in young and old rats," *J. Appl. Physiol.*, vol. 68, no. 1, pp. 130–134, 1990, doi: 10.1152/JAPPL.1990.68.1.130.

[91] U. Y, I. T, T. H, M. H, M. N, and S. H, "Effects of jump training on bone hypertrophy in young and old rats," *Int. J. Sports Med.*, vol. 16, no. 6, pp. 364–367, 1995, doi: 10.1055/S-2007-973021.

[92] B. KM, J. CR, T. RT, E. GL, F. PA, and D. HJ, "Aged bone displays an increased responsiveness to low-intensity resistance exercise," *J. Appl. Physiol.*, vol. 90, no. 4, pp. 1359–1364, 2001, doi: 10.1152/JAPPL.2001.90.4.1359.

[93] L. OV, S. H, J. J, P. I, K. P, and J. TL, "Pathogenesis of age-related osteoporosis: impaired mechano-responsiveness of bone is not the culprit," *PLoS One*, vol. 3, no. 7, Jul. 2008, doi: 10.1371/JOURNAL.PONE.0002540.

[94] R. CT, B. SD, and M. KJ, "Suppression of the osteogenic response in the aging skeleton," *Calcif. Tissue Int.*, vol. 50, no. 4, pp. 306–313, Apr. 1992, doi: 10.1007/BF00301627.

[95] T. CH, T. Y, and O. I, "Aging changes mechanical loading thresholds for bone formation in rats," *J. Bone Miner. Res.*, vol. 10, no. 10, pp. 1544–1549, 1995, doi: 10.1002/JBMR.5650101016.

[96] M. E. Lynch *et al.*, "Cancellous bone adaptation to tibial compression is not sex dependent in growing mice," *J. Appl. Physiol.*, vol. 109, no. 3, p. 685, Sep. 2010, doi: 10.1152/JAPPLPHYSIOL.00210.2010.

[97] C. PI, G. NJ, M. RW, and C. JE, "Age-related changes in resorption cavity characteristics in human trabecular bone," *Osteoporos. Int.*, vol. 1, no. 4, pp. 257–261, Sep. 1991, doi: 10.1007/BF03187471.

[98] E. EF, L. B, V. A, R. J, and K. M, "Hormone replacement therapy prevents osteoclastic hyperactivity: A histomorphometric study in early postmenopausal women," *J. Bone Miner. Res.*, vol. 14, no. 7, pp. 1217–1221, 1999, doi: 10.1359/JBMR.1999.14.7.1217.

[99] R. BL *et al.*, "A population-based assessment of rates of bone loss at multiple skeletal sites: evidence for substantial trabecular bone loss in young adult women and men," *J. Bone Miner. Res.*, vol. 23, no. 2, pp. 205–214, Feb. 2008, doi: 10.1359/JBMR.071020.

[100] A. O, A. F, and S. MB, "Age-related changes in physicochemical properties of mineral crystals are related to impaired mechanical function of cortical bone," *Bone*, vol. 34, no. 3, pp. 443–453, Mar. 2004, doi: 10.1016/J.BONE.2003.11.003.

[101] M. P *et al.*, "Osteocytic canalicular networks: morphological implications for altered mechanosensitivity," *ACS Nano*, vol. 7, no. 9, pp. 7542–7551, Sep. 2013, doi: 10.1021/NN401360U.

[102] T.-L. LM *et al.*, "Degeneration of the osteocyte network in the C57BL/6 mouse model of aging," *Aging (Albany. NY).*, vol. 9, no. 10, pp. 2187–2205, 2017, doi: 10.18632/AGING.101308.

[103] K. T. ML, A. JR, T. AE, and B. TW, "The osteocyte," *Int. J. Biochem. Cell Biol.*, vol. 36, no. 1, pp. 1–8, 2004, doi: 10.1016/S1357-2725(03)00241-3.

[104] T. EA, "Electron microscopic study of bone surface changes during aging. The loss of cellular control and biofeedback," *J. Gerontol.*, vol. 33, no. 2, pp. 163–177, 1978, doi: 10.1093/GERONJ/33.2.163.

[105] D. . Ortner, "Aging effects on osteon remodeling," *Calcif. Tissue Res.*, vol. 18, pp. 27–36, 1975.

[106] A. Franciscus Van Tol *et al.*, "The mechanoresponse of bone is closely related to the osteocyte lacunocanalicular network architecture," doi: 10.1073/pnas.2011504117/-/DCSupplemental.

[107] D. Shiba *et al.*, "Development of new experimental platform 'MARS'-Multiple Artificial-gravity Research System-to elucidate the impacts of micro/partial gravity on mice," doi: 10.1038/s41598-017-10998-4.

[108] M. Gerbaix *et al.*, "One-month spaceflight compromises the bone microstructure, tissue-level mechanical properties, osteocyte survival and lacunae volume in mature

mice skeletons OPEN," doi: 10.1038/s41598-017-03014-2.

[109] A. Shipov, A. Sharir, E. Zelzer, J. Milgram, E. Monsonego-Ornan, and R. Shahar, "The influence of severe prolonged exercise restriction on the mechanical and structural properties of bone in an avian model," *Vet. J.*, vol. 183, no. 2, pp. 153–160, 2010, doi: 10.1016/j.tvjl.2008.11.015.

[110] B. M. W. Haisheng Yang, Anne Seliger, Michael Thelen, Wing Lee Chan, Uwe Kornak, "Altered bone formation response to mechanical loading in a mouse model of the progeroid disorder gerodermia osteodyslastica," in *Orthopaedic Research Society*, 2015.

[111] L. I. Al-Gazali, L. Sztriha, F. Skaff, and D. Haas, "Gerodermia osteodysplastica and wrinkly skin syndrome: Are they the same?," *Am. J. Med. Genet.*, vol. 101, no. 3, pp. 213–220, Jul. 2001, doi: 10.1002/AJMG.1352.

[112] A. Nanda *et al.*, "Gerodermia osteodysplastica/wrinkly skin syndrome: Report of three patients and brief review of the literature," *Pediatr. Dermatol.*, vol. 25, no. 1, pp. 66–71, 2008, doi: 10.1111/j.1525-1470.2007.00586.x.

[113] H. C. Hennies *et al.*, "Gerodermia osteodysplastica is caused by mutations in SCYL1BP1, a Rab-6 interacting golgin," *Nat. Genet.*, vol. 40, no. 12, pp. 1410–1412, Dec. 2008, doi: 10.1038/ng.252.

[114] A. Rajab *et al.*, "Geroderma osteodysplasticum hereditaria and wrinkly skin syndrome in 22 patients from Oman," *Am. J. Med. Genet. Part A*, vol. 146A, no. 8, pp. 965–976, Apr. 2008, doi: 10.1002/ajmg.a.32143.

[115] J. Egerer *et al.*, "GORAB Missense Mutations Disrupt RAB6 and ARF5 Binding and Golgi Targeting," *J. Invest. Dermatol.*, vol. 135, no. 10, pp. 2368–2376, Oct. 2015, doi: 10.1038/JID.2015.192.

[116] T. M. Witkos *et al.*, "GORAB scaffolds COPI at the trans-Golgi for efficient enzyme recycling and correct protein glycosylation," doi: 10.1038/s41467-018-08044-6.

[117] W. Lee Chan *et al.*, "Impaired proteoglycan glycosylation, elevated TGF-β signaling, and abnormal osteoblast differentiation as the basis for bone fragility in a mouse model for gerodermia osteodysplastica," 2018, doi: 10.1371/journal.pgen.1007242.

[118] H. Yang *et al.*, "Examining tissue composition, whole-bone morphology and

mechanical behavior of GorabPrx1 mice tibiae: A mouse model of premature aging," *J. Biomech.*, vol. 65, pp. 145–153, 2017, doi: 10.1016/j.jbiomech.2017.10.018.

[119] W. W. Victoria Schemenz, André Gjardy, Fereshteh Falah Chamasemani, Alexander van Tol, Paul Roschger, Peter Fratzl, Roland Brunner, Richard Weinkamer, Bettina M. Willie, "Correlations between the osteocyte network and its surrounding matrix in newly formed bone," in *European Calcified Tissue Society*, 2019.

[120] J. Klein-Nulend *et al.*, "Sensitivity of osteocytes to biomechanical stress in vitro," *FASEB J.*, vol. 9, no. 5, pp. 441–445, Mar. 1995, doi: 10.1096/FASEBJ.9.5.7896017.

[121] P. S. Vezeridis, M. Semeins, Q. Chen, and J. Klein-Nulend, "Osteocytes subjected to pulsating fluid flow regulate osteoblast proliferation and differentiation," 2006, doi: 10.1016/j.bbrc.2006.07.146.

[122] S. Djien Tan, T. J. De Vries, A. M. Kuijpers-Jagtman, C. M. Semeins, V. Everts, and J. Klein-Nulend, "Osteocytes subjected to fluid flow inhibit osteoclast formation and bone resorption," 2007, doi: 10.1016/j.bone.2007.07.019.

[123] A. Vatsa, R. G. Breuls, C. M. Semeins, P. L. Salmon, T. H. Smit, and J. Klein-Nulend, "Osteocyte morphology in fibula and calvaria - Is there a role for mechanosensing?," *Bone*, vol. 43, no. 3, pp. 452–458, Sep. 2008, doi: 10.1016/j.bone.2008.01.030.

[124] R. P. van Hove *et al.*, "Osteocyte morphology in human tibiae of different bone pathologies with different bone mineral density - Is there a role for mechanosensing?," *Bone*, vol. 45, no. 2, pp. 321–329, Aug. 2009, doi: 10.1016/j.bone.2009.04.238.

[125] H. Hemmatian *et al.*, "Mechanical Loading Differentially Affects Osteocytes in Fibulae from Lactating Mice Compared to Osteocytes in Virgin Mice: Possible Role for Lacuna Size," *Calcif. Tissue Int. 2018 1036*, vol. 103, no. 6, pp. 675–685, Aug. 2018, doi: 10.1007/S00223-018-0463-8.

[126] S. K. Kola *et al.*, "Osteocyte lacunar strain determination using multiscale finite element analysis," *Bone Reports*, vol. 12, Jun. 2020, doi: 10.1016/J.BONR.2020.100277.

[127] R. P. Main, M. E. Lynch, and C. H. Van Der Meulen, "In vivo tibial stiffness is maintained by whole bone morphology and cross-sectional geometry in growing female mice," doi: 10.1016/j.jbiomech.2010.06.019.

[128] T. Sugiyama, J. S. Price, and L. E. Lanyon, "Functional adaptation to mechanical loading in both cortical and cancellous bone is controlled locally and is confined to the loaded bones," *Bone*, vol. 46, no. 2, p. 314, Feb. 2010, doi: 10.1016/J.BONE.2009.08.054.

[129] Z. ZA *et al.*, "Optimizing tamoxifen-inducible Cre/loxp system to reduce tamoxifen effect on bone turnover in long bones of young mice," *Bone*, vol. 81, pp. 614–619, Dec. 2015, doi: 10.1016/J.BONE.2015.07.034.

[130] X. Z *et al.*, "Low-Dose Tamoxifen Induces Significant Bone Formation in Mice," *JBMR plus*, vol. 5, no. 3, Mar. 2021, doi: 10.1002/JBM4.10450.

[131] M. Thelen, "Altered bone formation response to mechanical loading in a mouse model of the progeroid disorder gerodermia osteodysplastica," Berlin Technical University, Germany, 2018.

[132] M. K *et al.*, "Quantification of 3D microstructural parameters of trabecular bone is affected by the analysis software," *Bone*, vol. 142, Jan. 2021, doi: 10.1016/J.BONE.2020.115653.

[133] "Breeder farms," Accessed: Jul. 23, 2021. [Online]. Available: www.saskegg.ca.

[134] M. . Gentle, "Pain in birds," vol. 1, pp. 235–247, 1992.

[135] M. A. F. Nasr, J. Murrell, L. J. Wilkins, and C. J. Nicol, "The effect of keel fractures on egg-production parameters, mobility and behaviour in individual laying hens," *Anim. Welf.*, vol. 21, no. 1, pp. 127–135, Feb. 2012, doi: 10.7120/096272812799129376.

[136] M. A. Mccoy and G. A. C. Reilly, "Research in Veterinary Science," vol. 60, pp. 185–186, 1996.

[137] M. A. F. Nasr, J. Murrell, and C. J. Nicol, "The effect of keel fractures on egg production, feed and water consumption in individual laying hens," *Br. Poult. Sci.*, vol. 54, no. 2, pp. 165–170, 2013, doi: 10.1080/00071668.2013.767437.

[138] C. JR, B. DF, P. SF, and C. DR, "Activity of three muscles associated with the uncinate processes of the giant Canada goose Branta canadensis maximus," *J. Exp. Biol.*, vol. 208, no. Pt 5, pp. 849–857, Mar. 2005, doi: 10.1242/JEB.01489.

[139] C. LP, "The skeletal kinematics of lung ventilation in three basal bird taxa (emu, tinamou, and guinea fowl)," *J. Exp. Zool. A. Ecol. Genet. Physiol.*, vol. 311, no. 8, pp.

586–599, Oct. 2009, doi: 10.1002/JEZ.501.

[140] A. A. Biewener, W. . Corning, and B. W. Tobalske, “In vivo pectoralis muscle force-length behavior during level flight in pigeons,” *Exp. Biol.*, vol. 201, pp. 3293–3307, 1998.

[141] S. Hurwitz, “Calcium metabolism of pullets at the onset of egg production, as influenced by dietary calcium level,” *Poult. Sci.*, vol. 43, pp. 1462–1472, 1964.

[142] H. HA, B. WM, R. GN, and B. RJ, “Histomorphometric bone properties of sexually immature and mature White Leghorn hens with evaluation of fluorochrome injection on egg production traits,” *Poult. Sci.*, vol. 72, no. 8, pp. 1537–1547, 1993, doi: 10.3382/PS.0721537.

[143] T. M. Casey-Trott, M. T. Guerin, V. Sandilands, S. Torrey, and T. M. Widowski, “Rearing system affects prevalence of keel-bone damage in laying hens: a longitudinal study of four consecutive flocks,” *Poult. Sci.*, vol. 96, no. 7, pp. 2029–2039, 2017, doi: 10.3382/ps/pex026.

[144] G. . Buckner, W. . Insko, A. . Henry, and E. . Wachs, “Rate of growth and calcification of the sternum of male and female New Hampshire chickens,” *Poult. Sci.*, vol. 27, pp. 430–433, 1948.

[145] G. . Buckner, W. . Insko, A. . Henry, and E. . Wachs, “Rate of growth and calcification of the sternum of male and female New Hampshire chickens having crooked keels,” *Poult. Sci.*, vol. 28, pp. 289–292, 1949.

[146] T. Casey-Trott *et al.*, “Methods for assessment of keel bone damage in poultry,” *Poult. Sci.*, vol. 94, no. 10, pp. 2339–2350, 2015, doi: 10.3382/ps/pev223.

[147] W. D, V. A, H. H, H.-T. M, and D. O, “Macroscopic and histopathological alterations of foot pads of laying hens kept in small group housing systems and furnished cages,” *Br. Poult. Sci.*, vol. 47, no. 5, pp. 533–543, Oct. 2006, doi: 10.1080/00071660600963099.

[148] B. Scholz, S. Ronchen, H. Hamann, M. Hewicker-Trautwein, and O. Distl, “Keel bone condition in laying hens: a histological evaluation of macroscopically assessed keel bones,” *Berl Munch Tierarztl Wochenschr*, vol. 121, no. 3, pp. 89–94, 2008.

[149] B. Rodenburg, F. Tuyttens, K. De Reu, and S. B, “Welfare assessment of laying hens

in furnished cages and non-cage systems: An on-farm comparison," *Anim. Welf.*, vol. 17, no. 4, pp. 363–373, 2008.

[150] S. Käppeli, S. G. Gebhardt-Henrich, E. Fröhlich, A. Pfulg, H. Schäublin, and M. H. Stoffel, "Effects of housing, perches, genetics, and 25-hydroxycholecalciferol on keel bone deformities in laying hens," *Poult. Sci.*, vol. 90, no. 8, pp. 1637–1644, Aug. 2011, doi: 10.3382/PS.2011-01379.

[151] P. Y. Hester, S. A. Enneking, B. K. Haley, H. W. Cheng, M. E. Einstein, and D. A. Rubin, "The effect of perch availability during pullet rearing and egg laying on musculoskeletal health of caged White Leghorn hens," *Poult. Sci.*, vol. 92, no. 8, pp. 1972–1980, Aug. 2013, doi: 10.3382/PS.2013-03008.

[152] M. T. Petrik, M. T. Guerin, and T. M. Widowski, "On-farm comparison of keel fracture prevalence and other welfare indicators in conventional cage and floor-housed laying hens in Ontario, Canada," *Poult. Sci.*, vol. 94, no. 4, pp. 579–585, 2014, doi: 10.3382/ps/pev039.

[153] I. Thøfner, H. P. Hougen, C. Villa, N. Lynnerup, and J. P. Christensen, "Pathological characterization of keel bone fractures in laying hens does not support external trauma as the underlying cause," *PLoS One*, vol. 15, no. 3, 2020, doi: 10.1371/journal.pone.0229735.

[154] M. M. Beck and K. K. Hansen, "Role of estrogen in avian osteoporosis," in *Poultry Science*, Feb. 2004, vol. 83, no. 2, pp. 200–206, doi: 10.1093/ps/83.2.200.

[155] T. M. Casey-Trott, D. R. Korver, M. T. Guerin, V. Sandilands, S. Torrey, and T. M. Widowski, "Opportunities for exercise during pullet rearing, Part II: Long-term effects on bone characteristics of adult laying hens at the end-of-lay," *Poult. Sci.*, vol. 96, no. 8, pp. 2518–2527, Aug. 2017, doi: 10.3382/ps/pex060.

[156] R. C, B. S, S. A, and T. MJ, "A Reliable Method to Assess Keel Bone Fractures in Laying Hens From Radiographs Using a Tagged Visual Analogue Scale," *Front. Vet. Sci.*, vol. 5, no. JUN, Jun. 2018, doi: 10.3389/FVETS.2018.00124.

[157] I. Vitienes *et al.*, "Aviary rearing enhances bone microstructure in Lohmann LSL-Lite and bone mass in Lohmann Brown Lite egg-laying hen pullets compared to conventional cage-rearing," in *ASBMR*, 2021.

[158] E. Ross, "Effect of Early Rearing Environment on Musculoskeletal Traits and

Proximate Composition in Laying Hen Pullets," 2021.

[159] A. Pufall, A. Harlander-Matauschek, M. Hunniford, and T. M. Widowski, "Effects of Rearing Aviary Style and Genetic Strain on the Locomotion and Musculoskeletal Characteristics of Layer Pullets," vol. 11, p. 634, 2021, doi: 10.3390/ani11030634.

[160] A. Pufall, "The effects of three styles of commercial rearing aviaries on the locomotion and musculoskeletal development of pullets. MSc. Diss. University of Guelph, Guelph, Canada," 2020.

[161] J. BE, T. BW, and D. KP, "The broad range of contractile behaviour of the avian pectoralis: functional and evolutionary implications," *J. Exp. Biol.*, vol. 214, no. Pt 14, pp. 2354–2361, Jul. 2011, doi: 10.1242/JEB.052829.